Geomorphology 266 (2016) 105–120

Contents lists available at ScienceDirect

Geomorphology

journal homepage: www.elsevier.com/locate/geomorph

Degradation of the Mitchell River fluvial megafan by alluvial gully erosion increased by post-European land use change, Queensland, Australia

J.G. Shellberg *, J. Spencer, A.P. Brooks, T.J. Pietsch

Australian Rivers Institute, Griffith University, Nathan, Queensland 4111, Australia

ARTICLE INFO

Article history:
Received 10 January 2016
Received in revised form 23 April 2016
Accepted 25 April 2016
Available online 29 April 2016

Keywords:
Alluvial gully erosion
Air photograph interpretation
OSL dating
Geomorphic thresholds

ABSTRACT

Along low gradient rivers in northern Australia, there is widespread gully erosion into unconfined alluvial deposits of active and inactive floodplains. On the Mitchell River fluvial megafan in northern Queensland, river incision and fan head trenching into Pleistocene and Holocene megafan units with sodic soils created the poten tial energy for a secondary cycle of erosion. In this study, rates of alluvial gully erosion into incipiently unstable channel banks and/or pre existing floodplain features were quantified to assess the influence of land use change following European settlement. Alluvial gully scarp retreat rates were quantified at 18 sites across the megafan using recent GPS surveys and historic air photos, demonstrating rapid increases in gully area of 1.2 to 10 times their 1949 values. Extrapolation of gully area growth trends backward in time suggested that the current wide spread phase of gullying initiated between 1880 and 1950, which is post European settlement. This is supported by young optically stimulated luminescence (OSL) dates of gully inset floodplain deposits, LiDAR terrain analysis, historic explorer accounts of earlier gully types, and archival records of cattle numbers and land management. It is deduced that intense cattle grazing and associated disturbance concentrated in the riparian zones during the dry season promoted gully erosion in the wet season along steep banks, adjacent floodplain hollows and precur sor gullies. This is a result of reduced native grass cover, increased physical disturbance of soils, and the concen tration of water runoff along cattle tracks, in addition to fire regime modifications, episodic drought, and the establishment of exotic weed and grass species. Geomorphic processes operating over geologic time across the fluvial megafan predisposed the landscape to being pushed by land used change across an intrinsically close geomorphic threshold towards instability. The evolution of these alluvial gullies is discussed in terms of their initiation, development, future growth, and stabilisation, and the numerous natural and anthropogenic factors influencing their erosion.

1. Introduction

Gully erosion is a global phenomenon, a major cause of severe land degradation, and an important source of sediment pollution that re duces water quality and degrades aquatic ecosystems (Lal, 1992; Poesen et al., 2003; Valentin et al., 2005). In northern Australia, there is widespread alluvial gully erosion (sensu Brooks et al., 2009) into un confined alluvial deposits on active and inactive floodplains and fluvial megafans (Simpson and Doutch, 1977; Payne et al., 1979; Condon, 1986; Biggs and Philip, 1995; Brooks et al., 2009; McCloskey, 2010; Sattar, 2011; Shellberg et al., 2013a, 2013b). Alluvial gullies eroding into large floodplain and megafan surfaces are a distinct end member along a continuum of gully form process associations that are different from colluvial hillslope gullies, soft rock badlands, and valley bottom cut and fill channels in semi confined floodplains (Brooks et al., 2009). Alluvial gully initiation and evolution can span across spatial and temporal scales in floodplain environments, from small anthropo genically enhanced alluvial gullies (e.g., Vandekerckhove et al., 2001, 2003) to large alluvial gully tributaries cut into floodplains during sea level lowstands and inundated by backwater during highstands (e.g., Mertes and Dunne, 2008; Parker et al., 2008). The existence of al luvial gullies indicates that large floodplains and fluvial megafans are not consistently depositional environments through time, but rather temporary stores of sediment along fluvial process domains (Schumm, 1977) that are subject to erosion cell dynamics (Pickup, 1985, 1991) at a variety of spatial and temporal scales.

On the 31,000 km^2 Mitchell River fluvial megafan on Cape York Peninsula in northern Queensland (Fig. 1), a minimum area of 12,900 ha of alluvial gullying and 5560 km of active gully front length were mapped using remote sensing (Brooks et al., 2009; Fig. 2). These areas of de vegetated eroded sub soils were concentrated in dispersible floodplain soils adjacent to incised main channels, and covered 0.4% of the megafan area and up to 10% of the local flood plain area. Using preliminary head scarp retreat data (GPS) from 2005 to 2007 at distributed gullies, along with scarp height and pe rimeter measurements, Brooks et al. (2008) estimated that these

* Corresponding author at: 4.27 Building N78, 170 Kessels Road, Nathan, Queensland 4111, Australia.
E-mail address: j.shellberg@griffith.edu.au (J.G. Shellberg).

http://dx.doi.org/10.1016/j.geomorph.2016.04.021
0169-555X/

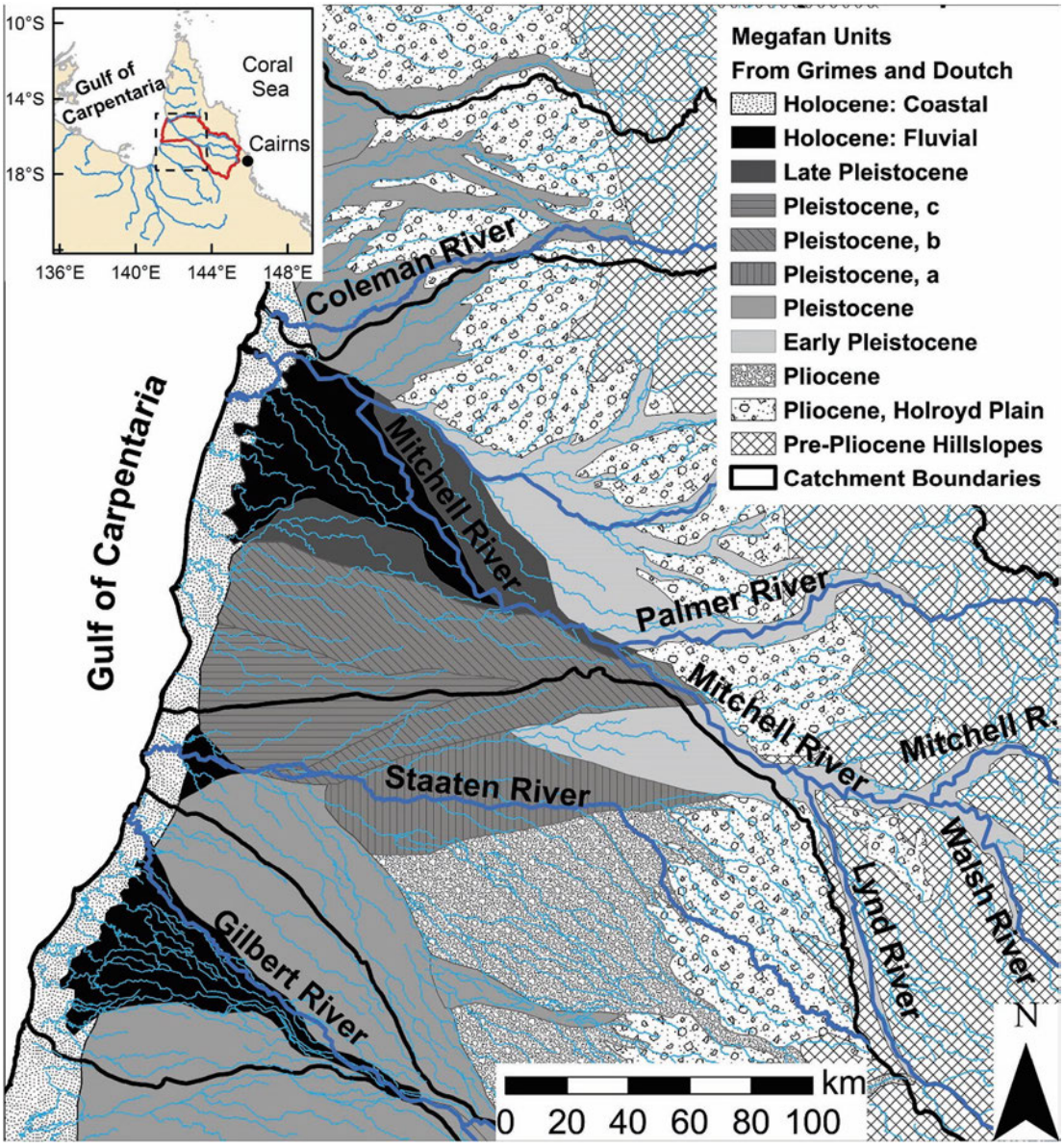

Fig. 1. Location and evolution of the Mitchell and Gilbert megafans from the Pliocene to Holocene (modified from Grimes and Doutch, 1978). The inset map of northern Queensland, Australia, shows the large map extent and the Mitchell catchment boundary.

gullies erode ~5 Mt yr^{-1} of alluvial soil from the megafan. Shellberg et al. (2013b) measured sediment yields of 89 to 363 t ha^{-1} yr^{-1} (2009 2010) at a stream gauge in a 33 ha gullied catchment (WPGC2a this study) on the Mitchell megafan. The degree to which these high erosion rates represent natural or human accelerated con ditions is an important research question, toward which this current study will provide supporting data. Since soil erosion threatens the sustainability of the local cattle industry, aquatic ecosystems and the cultural use of water bodies, understanding rates of gully erosion pre and post European settlement is important to define past human land use impacts and the sensitivity of the landscape to fur ther development.

Savanna catchments across northern Australia have undergone major land use changes from traditional Aboriginal management to widespread cattle grazing on unimproved rangelands since European settlement in the 1800s. Major alterations in grass cover, woodland thickening, exotic vegetation species, and fire regimes have resulted (Neldner et al., 1997; Fensham and Skull, 1999; Crowley and Garnett, 1998, 2000; Sharp and Whittaker, 2003; Bowman et al., 2004; Sharp and Bowman, 2004). Many assessments have documented, but not fully quantified, changes in sheet and gully erosion and sediment yield as a result of cattle grazing and/or European settlement in northern Australia (Medcalff, 1944; Payne et al., 1979; Condon, 1986; Wasson et al., 2002, 2010; Bartley et al., 2007, 2010; McCloskey, 2010; Hancock and Evans, 2010). Other sediment tracing studies in northern Australia have shown that current sediment loads are dominated by sub surface erosion (typically >90%) from primarily gully erosion, channel erosion, deep rilling and scalded soils (Hughes et al., 2009; Caitcheon et al., 2012; Wilkinson et al., 2013; Hancock et al., 2014; Olley et al., 2013); but to date few studies have looked at how these rates and processes of erosion have changed through time. Elsewhere in south eastern Australia, sediment yields clearly increased from accel erated soil, gully, and channel erosion associated with post European land use (Condon et al., 1969; Eyles, 1977; Wasson and Galloway, 1986; Pickup, 1991; Prosser and Winchester, 1996; Brooks and Brierley, 1997; Wasson et al., 1998; Fanning, 1999; Olley and Wasson, 2003; Rustomji and Pietsch, 2007).

The main objectives of this study were to investigate the growth rates of alluvial gullies and their evolution over time, and the stability of floodplain features and their threshold response to disturbance.

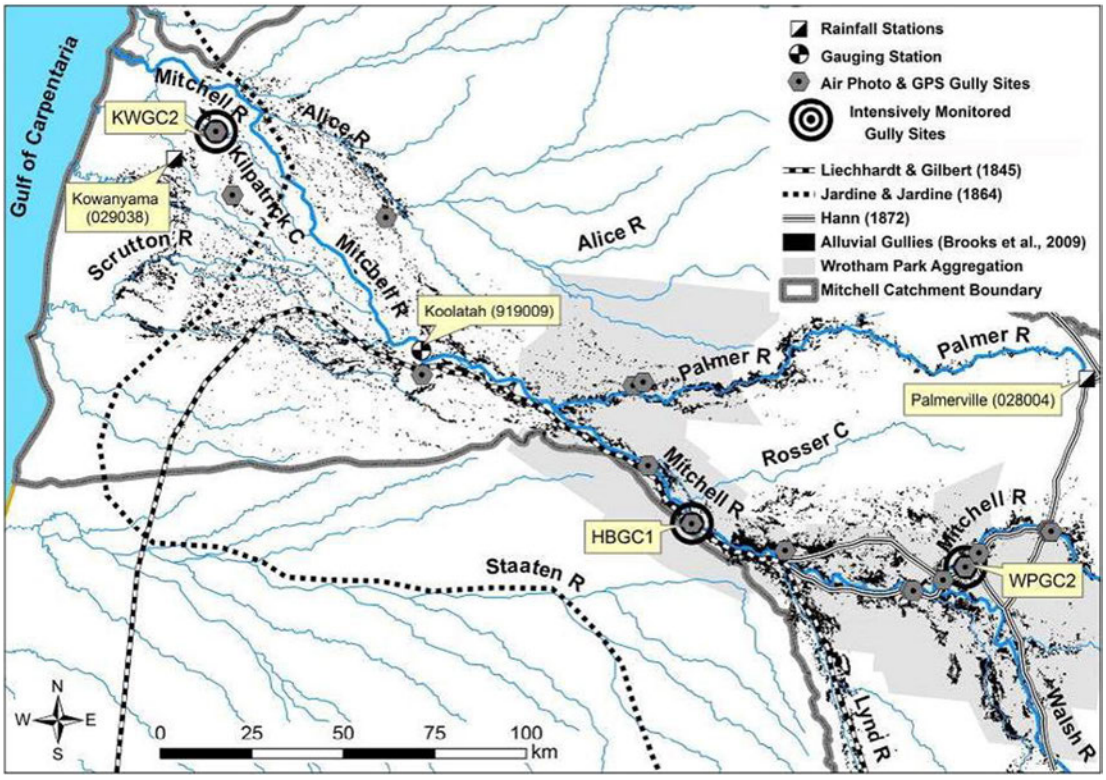

Fig. 2. Study area, gully sites, and monitoring stations along the lower Mitchell River fluvial megafan, along with the distribution of alluvial gullies, tracks of European explorers, and the extent of the Wrotham Park Aggregation cattle station. Several gully site symbols are hidden due to close proximity to others.

More specific research objectives were to 1) quantify how alluvial gully erosion rates have changed over different time scales along the Mitchell River fluvial megafan, 2) develop projections of gully erosion growth and duration into the future, 3) examine the form and evolution of allu vial gullies using Light Detection and Ranging (LiDAR) terrain analysis, 4) interpret early European explorer observations and potential post European land use impacts from settlement, 5) discuss the stability of floodplains and fluvial megafans influenced by natural and anthropo genic factors, and 6) describe a threshold response to disturbance the widespread initiation of alluvial gully erosion.

2. Regional setting and land use history

The Mitchell River fluvial megafan (31,000 km^2) in northern Queensland, Australia, consists of nested fluvial fans (>150 km in radi us) and river floodplains concentrated in the lower half of the Mitchell River catchment (71,630 km^2; Brooks et al., 2009). Major geomorphic units of the megafan were deposited from the Pliocene to the Holocene, but were especially active in the late Pleistocene during major sedimen tation periods (Galloway et al., 1970; Grimes and Doutch, 1978; Nanson et al., 1992; Fig. 1). Sea levels in the Gulf of Carpentaria, at the mouth of the Mitchell River, reached their minimum of 120 m below the present level during the late Pleistocene (~18,000 years ago), rose to their Holocene maximum of 1.5 m above the present level at 5500 years ago, and have since fallen to their present level (Chappell et al., 1982; Chivas et al., 2001). The current tidal range is 2 3 m in the Mitchell estuary, which extends 20 km inland along the 350 km total length of the Mitchell fluvial megafan.

During the very late Pleistocene and Holocene, river incision and fan head trenching into the fluvial megafan, and backfilled floodplain units upstream, occurred as the likely combined result of base level changes, reductions in sediment supply, and climate variability (Kershaw, 1978; Chappell et al., 1982; Nanson et al., 1992). This incision shifted the hydrologic apex of the megafan from near the Lynd River confluence (Pleistocene apex) to below the Palmer River confluence (Holocene apex of the Mitchell fan delta) (Figs. 1, 2). More recently, the active distributaries of the Holocene fan delta and deltaic estuary have prograded into the Gulf of Carpentaria during the last 5500 years (Nanson et al., 2013). River incision into both Pleistocene and Holocene megafan units at different times increased the local relative relief and potential energy between the river channel thalweg and high floodplain (Brooks et al., 2009; Shellberg et al., 2013a), which increased the possi bility of secondary cycles of erosion (sensu Pickup, 1985) by alluvial gully erosion initiating at steep channel banks.

A majority of alluvial gullies are located within 4 km of main creek and river channels, and are concentrated in the upstream incised sec tions of the Pleistocene megafan where relative relief is greatest (Brooks et al., 2009) (Fig. 2). Pleistocene high floodplains proximal to the river channel are dominated by fine grained (fine sand, silt and clay) dispersible sodic soils with high percentages of exchangeable sodi um (Isbell et al., 1968; Galloway et al., 1970; Shellberg et al., 2013a). Alluvial gullies are also widespread along channel banks and floodplains of the active Holocene fan, albeit of reduced density and size due to lower relief and less weathered soils (Biggs and Philip, 1995)(Fig. 2). Large portions of distal Pleistocene megafan units (Fig. 1) are less active currently in terms of erosion and deposition due to reduced connectiv ity to main river channels, low relief, and increased clay content in soils.

The Mitchell River catchment currently has a monsoonal, wet dry tropical climate that receives >80% of its annual rainfall and river runoff from December to March. Annual rainfall in the lower catchment aver ages 1015 mm and varies between 500 and 2000 mm (ABOM, 2015) (Fig. 3a). Storm rainfall intensity and erosivity are moderately high (Shellberg et al., 2013a), as are potential (1700 to 2000 mm yr^{-1}) and actual (600 to 900 mm yr^{-1}) evapotranspiration (ABOM, 2015). Inter annual rainfall totals are variable in the Mitchell catchment, with multi year wet and dry phases that are influenced by cycles of El Niño Southern Oscillation (ENSO) and Interdecadal Pacific Oscillation (IPO) (Lough, 1991; Risbey et al., 2009) (Fig. 3b).

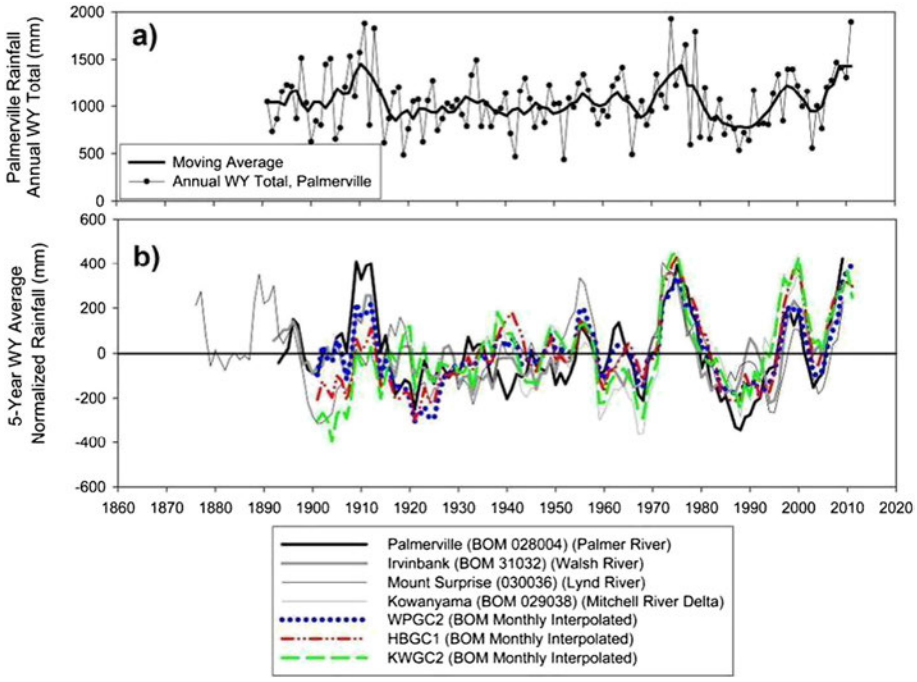

Fig. 3. Historic trends of a) rainfall totals by water year (WY, Oct to Sept) for Palmerville Station (028004) in the Mitchell catchment (Fig. 2), and b) normalized rainfall totals (WY, 5-year moving average divided by mean) for catchment rainfall stations and interpolated data (ABOM monthly data, 1900–2011; Jones et al., 2009) for main gully sites (Fig. 2).

Aboriginal people have managed the Mitchell catchment for tens of thousands of years (Sharp, 1934). The first European explorers traveled through the catchment in the mid 1800s (Gilbert, 1845; Leichhardt, 1847; Jardine and Jardine, 1867). In 1872, gold was discovered near Palmerville (Hann, 1872) (Fig. 2). Pastoralism followed soon after across the savanna woodlands of the lower catchment. The number of introduced cattle increased to >40,000 head over the subsequent 140 years (Fig. 4), as reported in historic archives of herd data for the Wrotham Park Aggregation cattle station (9973 km^2; Fig. 2; Edye and Gillard, 1985; Arnold, 1997; QSA, 2008), which now consists of Wrotham Park, Gamboola, Gamboola South, Highbury, and Drumduff Stations. These herd size trends generally followed total cattle numbers across Queensland (Fig. 2; ABS, 2008). Low density cattle grazing (1 beast per 20 ha on average) across open range has been the predominant land use (Edye and Gillard, 1985; Arnold, 1997). However, cattle density (>1 beast per 8 ha) and impacts were concentrated along river, creek, and lagoon frontages, where animals congregated for water and feed during the long dry season and cattle drives (QSA, 2008). Over time, thousands of kilometers of fences have been installed across the megafan, but primarily are used to divide very large paddocks and seldom to protect waterways or river frontage from grazing.

All of the early European explorers along the lower Mitchell River (Gilbert, 1845; Leichhardt, 1847; Jardine and Jardine, 1867; Hann, 1872) anecdotally described fluvial features including floodplain drainage 'hollows', 'gullies' and 'creeks' near the 'steep banks' of the rivers. Their definitions and use are open to interpretation (Shellberg, 2011). For example, Leichhardt (1847) wrote that "*the* [*floodplain*] *was interrupted by gullies and deep creeks*, *which* [*were*] *the outlets of the waters collecting on the* [*floodplain*]". Gilbert (1845) wrote that they had "*to keep well back* [*from the river*] *to avoid the deep gullies frequent on the immediate banks*". Hann (1872) wrote that "*the many gullies and broken country made it impossible to travel* [*by horse along the river bank*]". Gilbert (1845) and Jardine and Jardine (1867) also used the term 'broken' country in contrast to open flats that were easy to ride horses through. The explorers' anecdotal observations provide a background for more in depth geomorphic quantification and interpretation of gully evolution along the Mitchell fluvial megafan.

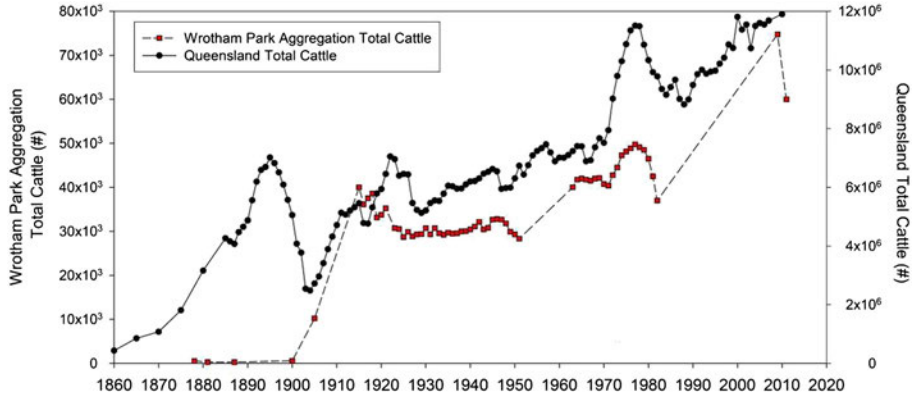

Fig. 4. Historic archive trends in reported cattle numbers for 1) the State of Queensland (ABS, 2008), and 2) the historic Wrotham Park Aggregation cattle station (Fig. 2) on the Mitchell megafan (QSA, 2008; Edye and Gillard, 1985; Arnold, 1997; pers. Comm. with station managers, 2008).

3. Methods

3.1. Recent and historic gully erosion rates and area expansion

Across the Mitchell River megafan, a representative subset of 18 alluvial gullies were selected for analysis based on the mapped spatial distribution of gullies and field reconnaissance of randomly selected sites (Brooks et al., 2008, 2009; Fig. 2). Gullies initiated by fence lines and roads were not included as study sites. Three gully complexes (WPGC2, HBGC1, and KWGC2) on main channel banks were selected as intensively monitored sites on the upper, middle, and lower sections of the megafan along a continuum of geologic age (Pleistocene to Holocene), river incision and local relative relief decreasing in the downstream direction (Brooks et al., 2009), which are reported on here and elsewhere (Shellberg, 2011; Shellberg et al., 2013a, 2013b).

Recent annual surveys (2005 2010) of alluvial gully fronts (scarps) were conducted at the 18 study sites (Fig. 2) using differential GPS (Trimble with Omnistar High Precision). In combined total, ~50,040 m of scarp front were surveyed with GPS each year. Horizontal accuracy depended on signal strength and vegetation cover, but was typically 10 15 cm and always <50 cm. Error margins in gully area were calculated by buffering each survey line by ±0.50 m, with any area changes within the buffer overlap omitted from final calculations. The average linear erosion rate (m yr^{-1}) for each gully for each year was calculated as the area of change (m^2) between any two survey years divided by the survey length (m) of active gully perimeter at the later time period.

Air photographs of the same sites were used to assess the historic location and rates of gully front erosion. The earliest photographs were from 1949 or 1955, with the average number of photos per site between 1949 and 2006 being 5 and ranging from 3 to 7. The photo scale ranged from 1:20,000 to 1:85,000, with the first (1949, 1:23,900) and last photos (2006, 1:20,000) having the largest scales. High resolution (2400 dpi) digital copies were clipped to the general gully area (<4 km^2). Photos were georectified backward through time in a GIS (e.g., Hughes et al., 2006), starting with GPS surveys and LiDAR data (where available) to rectify 2006 photos. For each photo, a minimum of six ground control points were used that were consistently identifiable between photos; these were most often large trees but also fence lines, roads, and stable fluvial features. A first order polynomial georectification was used along with a cubic convolution resampling of pixels (Hughes et al., 2006).

For each gully and photo year, the gully head scarp location was digitized from rectified photos. In total for the 18 sites, ~ 43,160 m of scarp front was digitized for each photo year. Error margins for the gully scarp location and gully area were estimated from the total root mean square errors (*RMSE*) for the rectified photos (e.g., Hughes et al., 2006), which averaged 1.39 m and ranged from 0.36 to 3.32 m. Repeat digitisation of scarp edges from photos indicated that scarps could be consistently located within ±2 3 m as compared to GPS and LiDAR surveys. Therefore, each digitized line was buffered by ±2 m if obtained from high resolution photos (<1:30,000) and ±3 m for coarser resolution photos (>1:30,000). Area changes within the buffer overlap were omitted from final calculations. Annual average linear erosion rates (m yr^{-1}) were calculated similar to GPS methods above.

The change in the bare eroded gully area over time (1949 2010) was determined for different sites using the combination of historic photo and recent GPS data. The zero area or starting point for each gully was located at the confluence of the gully channel with a mainstem river, lagoon, or large creek. In a few cases, the transition between bare gully complexes and their narrow outlet channels that traverse dense riparian zones could not be mapped using historic air photos, resulting in these areas being omitted from the analysis.

According to disturbance, response and relaxation theory (Schumm, 1977; Graf, 1977), it was initially hypothesized that increasing trends in gully area over time would follow negative exponential rates of change that are common in unstable channels (Graf, 1977; Simon, 1992; Rutherfurd et al., 1997; Wu et al., 2012). A modified negative exponential function was fitted to the data for each gully:

$$\frac{A}{A_0} \quad a + be^{(\ \ kt)} \tag{1}$$

where A is the exposed gully area at time t, A_0 is the initial gully area at $t = 0$, a and b are dimensionless coefficients determined by regression, k is a coefficient determined by regression that defines the rate of change in gully area over time, and t is the time (yr) since the initial starting point or the first air photograph. When k is very small the equation approaches linearity, as dictated by the data trend and goodness of fit determined by the coefficient of determination (r^2).

3.2. Past gully erosion chronologies from OSL dating

To quantify timing and rates of sediment deposition (and thus 'upstream' erosion) within gullies, alluvial sediment samples were collected in 2009 from vertical cut banks of incised outlet channels within two gully complexes (WPGC2 and HBGC1) (Fig. 2). Samples were dated using single grain optically stimulated luminescence (OSL) (Aitken, 1998; Olley et al., 2004; Pietsch, 2009). OSL dating was not conducted at KWGC2 because air photograph evidence clearly indicated that the gully erosion was <100 years old, and ^{14}C dating (not reported here) was used in a separate study to date recent tree colonization into the gully (Shellberg, 2011).

At both WPGC2 and HBGC1, a gully cross section was located for sampling downstream of the major gully erosion but upstream of river backwater conditions, to isolate gully outwash sediment. Major sedimentary units (i.e., Pleistocene megafan sediment and Holocene gully sediment) were defined in one or more vertical profiles along or near each cross section and sampled for OSL dating. Ten discrete OSL sediment samples at WPGC2 and four at HBGC1 were collected (Table 1). The measured OSL burial ages were used to interpret the timing of sediment deposition within the gullies, and infer erosion timing and gully evolution. In addition, the vertical distances between samples in a profile and the sample ages were used to estimate sedimentation rates for different sedimentary units, and thus infer changes in erosion rates over time.

Single grain OSL dating of quartz grains (180 212 μm) followed the techniques and instrumentation of Olley et al. (2004) and Pietsch (2009) to determine the burial age (years before present, BP, or the year of sampling in 2009) from the equivalent dose (D_e, Gy) the buried grain(s) received cumulatively over time and the total dose rate (D_r, Gy yr^{-1}) received from radiation in the surrounding environment. The dose rate was calculated from soil radionuclide activities measured using gamma spectrometry (Murray et al., 1987), using conversion factors from Stokes et al. (2003), and beta dose attenuation factors from Mejdahl (1979). For all samples, a long term average water content of 5 ± 5% was used for this seasonally dry climate. A modified single aliquot regenerative dose (SAR) protocol (Olley et al., 2004) was used to determine the dose response curve and D_e for each grain. Between 600 and 1700 single grains were analysed for each sample, with these yielding on average 6% that passed our commonly used acceptance criteria (see Pietsch, 2009; Pietsch et al., 2015). Overdispersed grain dose populations were observed in all cases, which we interpreted as being primarily a result of partial bleaching; hence burial doses were calculated using the minimum age model (and its unlogged variant for very low dose samples) with an assumed underlying overdispersion of the grain dose population immediately after burial of 10% (see Arnold et al., 2009; Galbraith and Roberts, 2012). For two samples (WP13 and WP07), the majority of grains acting as reliable dosimeters were observed to have doses in excess of the saturation point

Table 1
OSL sample ages (years before 2009) from WPGC2 and HBGC1. Radionuclide values (Bq kg $^{-1}$) were used to determine the dose rate, Grains is number of grains accepted for equivalent dose calculation and the number of grains analysed, D_e (Gy) is the equivalent dose, D_r (Gy kyr $^{-1}$) is the total dose rate, and *Age* (yr) is the burial age in years. Ages and uncertainties were rounded to the nearest 10 yrs when the age is <100 yrs, and 20 yrs where the age is between 100 and 1000 yrs.

Site	Code	Profile	Unit	Depth (cm)	^{238}U	^{226}Ra	^{210}Pb	^{232}Th	^{40}K	Grains (n)	D_e (Gy)	D_r (Gy kyr $^{-1}$)	*Age* (yr)
WPGC2a	WP-03	2	Ab	45	51.9 ± 2.9	49.8 ± 0.7	40.5 ± 3.6	75.7 ± 3.4	530.6 ± 12.2	49/1000	0.27 ± 0.03	3.67 ± 0.35	70 ± 15
WPGC2a	WP-04	2	Ac	65	52.9 ± 1.9	48.2 ± 0.6	42.7 ± 2.4	74.7 ± 1.5	510.9 ± 11.1	77/1300	0.27 ± 0.04	3.66 ± 0.35	70 ± 15
WPGC2a	WP-05	3	Aa	30	76.6 ± 2.4	92.6 ± 1.1	67.3 ± 3.0	88.8 ± 21.9	492.3 ± 10.6	56/1500	0.06 ± 0.03	3.95 ± 0.39	15 ± 10
WPGC2a	WP-07	3	C	75	54.1 ± 2.8	62.7 ± 0.9	49.1 ± 3.6	72.4 ± 10.0	689.6 ± 16.4	23/600	>150	4.38 ± 0.41	>35,000
WPGC2b	WP-10	5	A	50	50.9 ± 2.7	49.7 ± 0.7	41.9 ± 3.4	60.6 ± 14.1	553.8 ± 13.6	109/1700	0.36 ± 0.02	3.86 ± 0.34	90 ± 10
WPGC2b	WP-11	5	B	80	55.2 ± 2.1	48.9 ± 0.7	43.0 ± 2.7	72.2 ± 2.4	525.9 ± 12.1	77/1600	0.67 ± 0.04	3.71 ± 0.35	180 ± 20
WPGC2b	WP-12	5	B	120	55.7 ± 2.0	51.7 ± 0.7	46.5 ± 2.2	75.7 ± 0.9	564.2 ± 12.0	70/1200	2.00 ± 0.08	3.88 ± 0.36	515 ± 60
WPGC2b	WP-13	5	C	160	50.4 ± 1.6	45.8 ± 0.6	45.7 ± 2.2	82.2 ± 5.4	590.6 ± 12.4	87/1000	>150	3.94 ± 0.37	>35,000
WPGC2a	WP-19	7	A	51	80.3 ± 2.6	114.0 ± 1.4	79.3 ± 3.5	76.9 ± 11.9	596.2 ± 12.7	74/1300	0.49 ± 0.02	4.79 ± 0.47	100 ± 10
WPGC2a	WP-20	7	B	67	52.2 ± 2.5	50.9 ± 0.7	44.2 ± 2.7	74.4 ± 2.7	516.0 ± 11.9	59/1500	0.46 ± 0.02	3.68 ± 0.35	125 ± 20
HBGC1	HB-01	1	A	6	65.8 ± 2.1	58.2 ± 0.7	66.3 ± 2.6	92.6 ± 1.1	247.1 ± 5.6	68/1000	0.01 ± 0.005	3.64 ± 0.38	5 ± 5
HBGC1	HB-02	1	B	20	62.4 ± 2.2	59.4 ± 0.8	58.5 ± 2.5	95.4 ± 1.3	220.1 ± 5.3	71/1000	0.06 ± 0.02	3.48 ± 0.37	20 ± 10
HBGC1	HB-04	1	D	35	37.9 ± 1.4	30.2 ± 0.4	30.8 ± 1.6	45.2 ± 0.6	220.0 ± 5.1	77/1000	0.06 ± 0.01	2.17 ± 0.21	30 ± 10
HBGC1	HB-05	1	E	45	44.1 ± 1.6	38.0 ± 0.5	38.2 ± 1.9	58.0 ± 1.0	240.4 ± 5.5	94/1000	0.15 ± 0.01	2.57 ± 0.26	60 ± 10

of their respective growth curves. For these two samples, we used the average onset of saturation as an indicative minimum possible burial dose, and hence the ages thus calculated are taken as mini mum ages only.

3.3. Projections of future gully growth and duration

Future projections of gully growth at the three intensively moni tored gully sites (WPGC2, HBGC1, and KWGC2; Fig. 2) were assessed from over 50 longitudinal profiles of the channel thalweg elevation at each site extracted from Light Detection and Ranging (LiDAR) DEM data. These data were collected in 2008 and DEMs (1 m^2 grid) were gen erated from point data using the natural neighbour interpolation model. Each profile radiated out from the main channel along individual den dritic tributaries and extended through the gully scarp zone onto the flat terrain of the river high floodplain. Future projections of the spatial expansion of gully area were made by forward trending the slope of the outlet channel, common to all tributaries, through the scarp zone and into the uneroded alluvial plain. This assumes that the sand bed gully outlet channels are at an equilibrium slope or grade (sensu Mackin, 1948; Lane, 1955) due to abundant sand bed material supplied from gully scarp failure during monsoon rains (Brooks et al., 2009; Shellberg et al., 2013a, 2013b; Rose et al., 2015). It also assumes that over steepened scarp fronts will flatten over time toward a graded slope, due to the unconfined nature of the high floodplain. The ultimate erosion extent of the gully was located where the projected graded slope intersected the elevation of the relatively flat uneroded floodplain or the surface of another topographic feature. However, since the channel slope within each gully was a sinuous thalweg slope rather than a straight line valley slope, the calculated straight distance from the current scarp edge to the future estimated scarp endpoint was ad justed to a straight line valley distance by dividing this distance by the sinuosity of the outlet channel.

The form of gully area growth trajectories and trends into the future are unknown and could follow linear, negative exponential or other functions depending on internal gully evolution processes and/or future climatic forcing. Linear trends using 1949 2010 area data were initially used to estimate the minimum time when the gully scarp would reach a graded slope in all directions by projecting trends into the future until the relative gully area (A/A_0) spatially projected by the profile exten sions was reached. Negative exponential trends using 1949 2010 area data alternatively were used to project the time to reach a graded slope, assuming that expansion rates continue to relax over time as observed at many sites. Projection uncertainties of both approaches are discussed.

3.4. Analysing gully evolution from LiDAR data

The 2008 LiDAR DEMs (1 m^2 grid) were analysed to examine the form and evolution of alluvial gullies and floodplain hollows. A location for time substitution was adopted for alluvial gullies at differ ent stages of evolution (initiation, expansion, and stabilisation; Brooks et al., 2009). Cross section and longitudinal profile data extracted from LiDAR data were used to compare hollow and gully forms and possible evolution over time. Site HBGC1 was selected as a case study due to the presence of multiple forms of gullies and floodplain hollows, and having been passed directly by Leichhardt and Gilbert in 1845 (Fig. 2).

4. Results

4.1. Recent and historic gully erosion rates and area expansion

Recent GPS surveys (2005 2010) documented the more or less consistent annual growth rates of alluvial gully area (Fig. 5). However, linear erosion rates were variable within individual gully scarps, with the highest rates at distinct lobes or alcoves of water convergence (in planform) compared to inter lobe zones along more linear scarps (Fig. 5). Maximum retreat rates regularly exceeded 1 m yr^{-1}, with ex treme values >10 m yr^{-1} (Brooks et al., 2009; Shellberg et al., 2013a, 2013b). Inter lobe zones were more stable with rates <0.5 m yr^{-1}.

Historical air photographs documented the longer term growth of alluvial gullies, demonstrating that these gullies can consume large areas of floodplain margins consistently through time (Fig. 6). Early phases of gully growth were predominantly linear headward retreat. Subsequently, lateral widening expanded gully growth to develop amphitheatre shaped gully complexes that were as wide as they were long (Brooks et al., 2009) (Fig. 6).

Annual average scarp retreat rates varied by year, period, site, and measurement method (Fig. 7). The median rate of annual average scarp retreat (area change/scarp perimeter) from recent GPS surveys (2005 2010; 18 sites; 41 time steps; 50,040 m of scarp) was 0.23 m yr^{-1} compared to 0.37 m yr^{-1} from historic air photos (1949 2006; 18 sites; 58 time steps; 43,163 m of scarp). The historic air photos (1949 2006) vs. recent GPS (2005 2010) distributions were significantly different from each other ($p = 0.001$, $\alpha = 0.05$; non parametric Kruskal Wallis one way analysis of variance; Fig. 7). For additional analysis of the nature of the form of the gully growth model, the historical air photo period (1949 2006) was split into two periods (1949 1975 and 1975 2006) with equal sam ple sizes based on air photo availability. These two distributions were marginally different ($p = 0.058$, $\alpha = 0.05$). When the two pe riods of historical air photo (1949 1975 and 1975 2006) and the

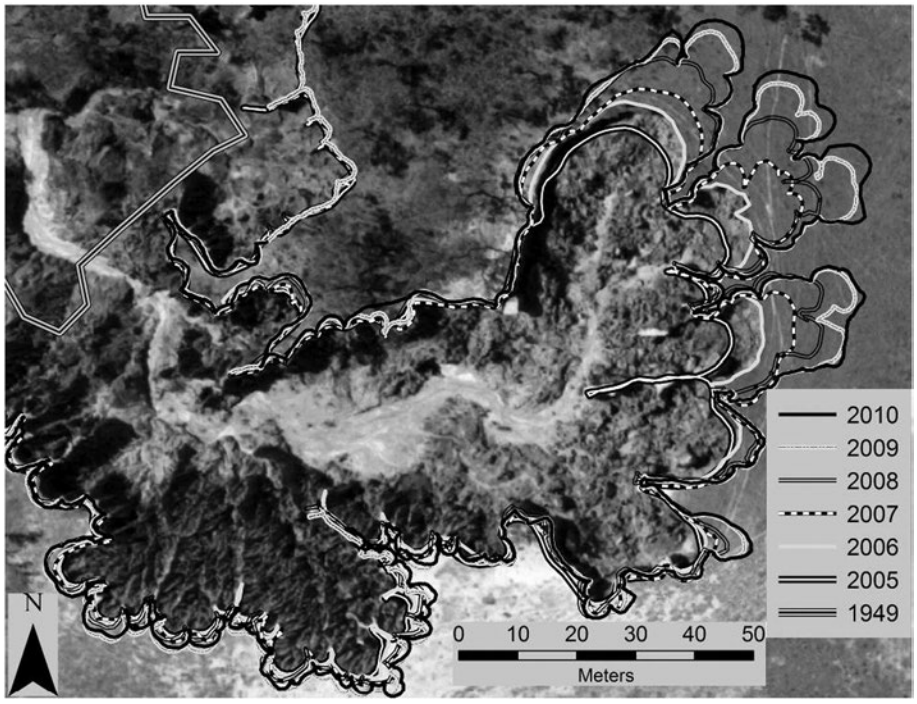

Fig. 5. Annual gully scarp location between 2005 and 2010 at WPGC3 measured using GPS, with 1949 position from historic air photo and recent 2006 photo in background.

period of recent GPS (2005 2010) were compared, the results were significantly different ($p < 0.001$; $\alpha = 0.05$; Fig. 7).

The combined scarp location data from historic air photos and recent GPS surveys showed progressive growth of all 18 gully complexes over time (Fig. 8a). Relative gully area (A/A_0) for individual gullies increased from 1.2 to 10 times their initial 1949 areas. Trend results were the same whether the recent GPS data were included or excluded from the histor ical air photo data. The estimated error in gully area for any given year was relatively small compared to the magnitude of area change over the 60 years (Fig. 8).

Fitting the negative exponential function to the combined data indi cated that erosion rates varied from negative exponential to near linear depending on the site. The values of the coefficient k (0.0007 to 0.0028) were small (near linear), but allowed for the exploration of the degree of linearity in the data without assuming a linear function. Values of r^2 were high (average $r^2 = 0.981$, range 0.872 to 0.999). Although many sites had declining growth rates over time (Fig. 8b), due to the low sam ple size (average 5, range 3 to 7) and short time frame (<60 years), linear and logarithmic functions also fit the data well (average $r^2 =$ 0.979 and 0.976, respectively).

Sites with the highest erosion rates (m yr^{-1}) and greatest relative expansion ($A/A_0 > \sim 2$) had the smallest k values in the exponential function, suggesting near linear areal expansion. Head scarp retreat was dominated by undercutting and mass failure of soil blocks at these sites (Brooks et al., 2009). For these fast growing gullies, extrapo lation of gully area growth trends backward in time ($A/A_0 \ll 1$) suggests that the time frame for initiation was between 1910 and 1950, i.e. after the introduction of cattle (Fig. 8a). Often these gullies had the most identifiable starting points near the banks of rivers or lagoons.

In contrast, sites with low erosion rates (m yr^{-1}) and small relative expansion ($A/A_0 < \sim 2$) had larger k values, suggesting non linear trends with rapid initial growth and slower growth over time. Head scarp retreat was dominated by direct rainfall and fluting and carving of the gully front face at these sites (Brooks et al., 2009). These slower growing gullies had less identifiable starting points and indeterminate initiation times before 1900, but consistent with the period of European settlement (Fig. 8b).

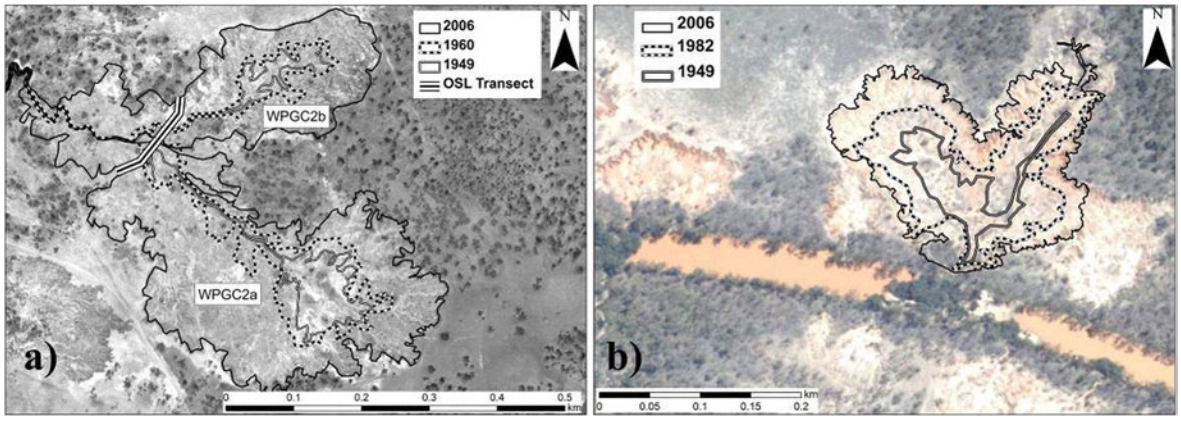

Fig. 6. Changes in gully scarp location from 1949 to 2006 at a) Wrotham Park (WPGC2) with the OSL cross-section location (see Fig. 10), and b) Highbury (HBGC2) where gully sediment infilled the previously free flowing lagoon channel between 1982 and 2006.

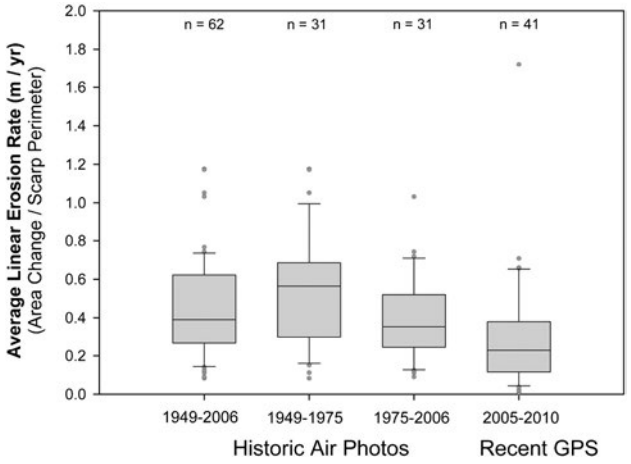

Fig. 7. Comparison of annual average linear erosion rates (area change/scarp perimeter, m yr ^{1}) measured from historic air photos and recent GPS surveys. Sample sizes (n) represent the total number of measurements between individual years (time steps) for all gullies within the overall time period. Boxes represent 25th, 50th, 75th percentiles, whiskers represent 5th and 95th percentiles, and points represent outliers.

4.2. Gully erosion chronologies from OSL dating

Measured OSL burial ages (Fig. 9; Table 1) were used to interpret the timing and rates of gully evolution before and after European settlement (circa 1872). At WPGC2 (Figs. 2 and 6a), OSL samples obtained from three vertical profiles (2, 3, and 5) located along a cross section transect through the lower gully (Fig. 10), with one additional nearby profile (7) (Table 1). Example radial plots of D_e data for profile 5 are included in Fig. 9. Profile 5 in WPGC2b consisted of three sedimentary units (Fig. 11). The lower Unit C consisted of massive indurated silt/clay deposited in the Pleistocene during the construction of the fluvial megafan (>35,000 yr BP; Table 1: WP13). Unit B was deposited above an unconformity with Unit C. Unit B was an indurated silty clay deposit that lack visible sedimentary structures, and infilled a floodplain hollow or swale on the surface of Unit C with silt, clay and organic material in a low energy environment (Fig. 10). The top of Unit B was the pre European soil surface (180 515 yr BP; Table 1: WP 11 to 12), as also indicated by a buried (in situ) tree which grew on top of Unit B (Fig. 11a). The laminated silt and Fe/Mn (ferricrete) nodules of Unit A were deposited following European settlement (90 yr BP; Table 1: WP 10) and eroded from sheet and/or shallow gully erosion in the upslope catchment.

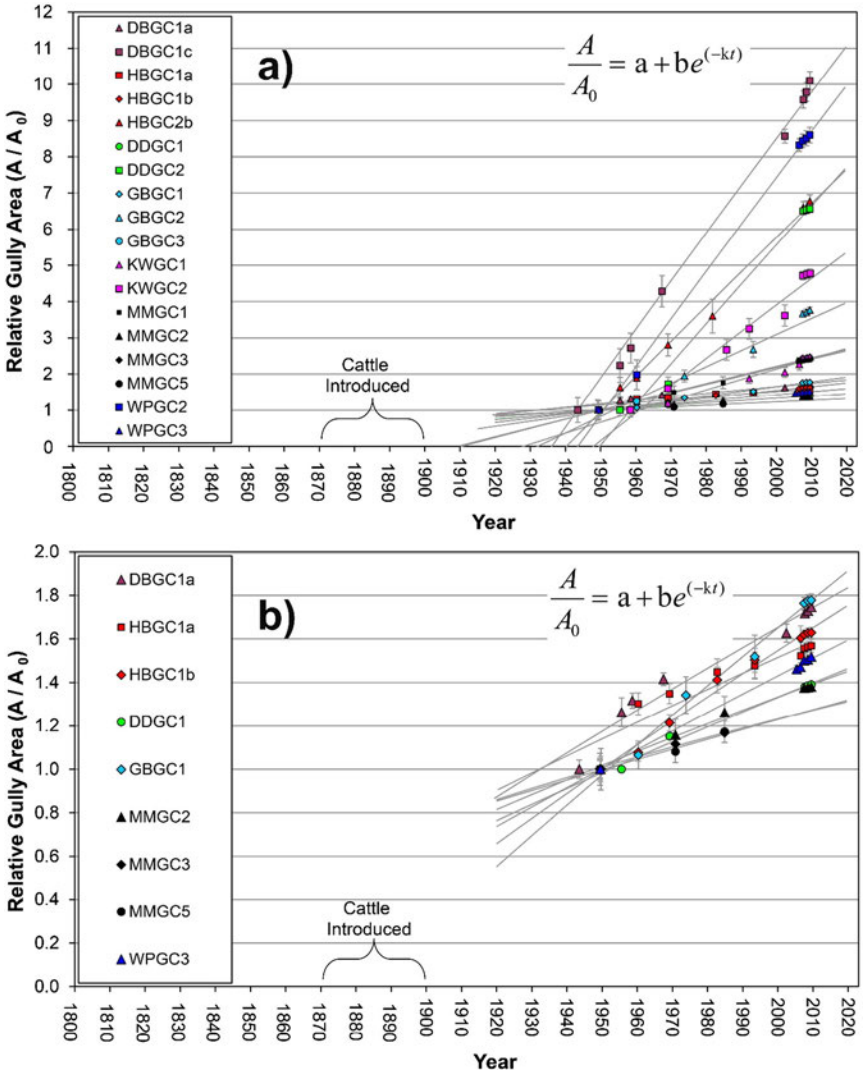

Fig. 8. Relative changes in gully area (A/A_0) over time for a) all 18 gully sites (Fig. 2), and b) a subset of 9 sites with $A/A_0 < 2$. A negative exponential function was fitted to the data using historical air photos (1949–2006) and recent GPS surveys (2005–2010). Error bars correlate to horizontal errors of ±2 to 3 m for historic photos and ±50 cm for recent GPS.

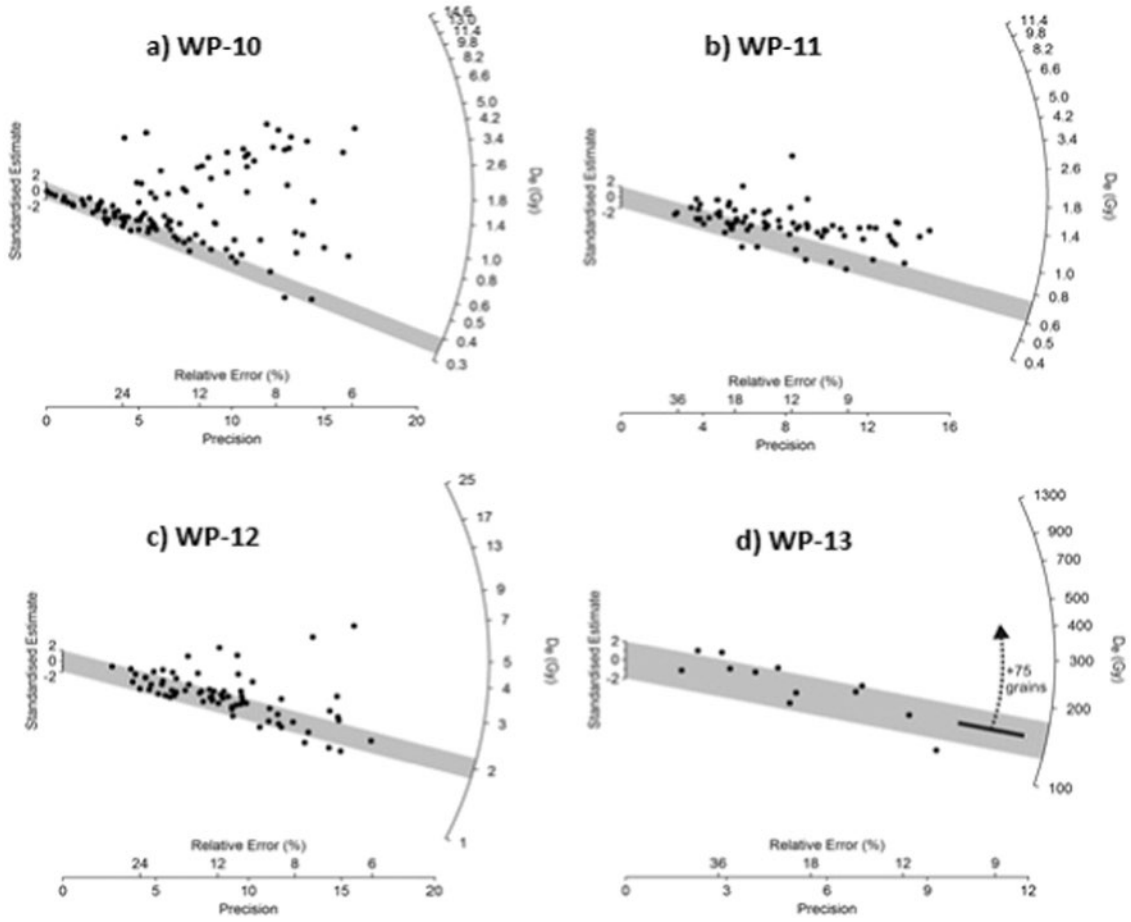

Fig. 9. Radial plots of equivalent dose (D_e) data for samples a) WP-10, b) WP-11, c) WP-12, and d) WP-13 at profile 5 at WPGC2b. The *x*-axis plots the relative standard error (%) and its reciprocal, precision, while the shaded area represents the 2σ confidence interval for the D_e estimate. For WP-13, 75 grains had doses at or above their respective saturation points of ~150 Gy, as indicated by dashed arrow.

At profile 7 upstream in WPGC2a, OSL data from a thinner section of unit A confirmed that its deposition initiated 100 yr BP (Table 1: WP 19) at the bottom of the unit and buried the older unit B immediately under neath (125 yr BP; Table 1: WP 20). At profiles 2 and 3 in WPGC2a (Fig. 10), the unconsolidated fill units Aa to Ac of small inset floodplains within the gully were deposited following European settlement (15 70 yr BP; Table 1: WP 03 to 05). These deposits overly a major uncon formity that was exposed by gully erosion cutting into the indurated Pleistocene sediments of unit C (>35,000 yr BP; Table 1: WP 07).

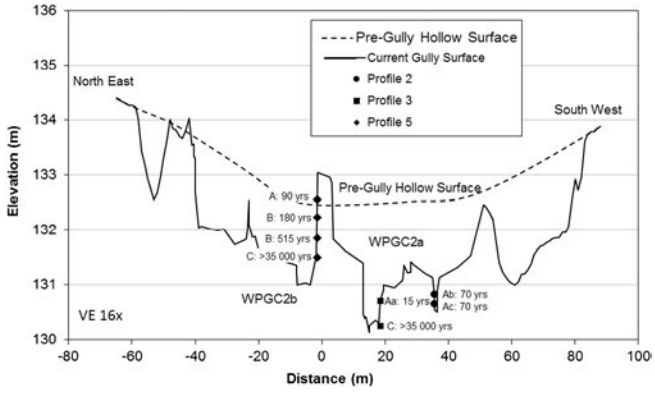

Fig. 10. Cross-sectional transect through WPGC2 with locations of vertical profiles, OSL sample locations, OSL ages (years BP), and the approximate location of the pre-gully hollow surface. See Fig. 6a for planform location.

These OSL data at WPGC2 demonstrate a complex response to gully evolution from initial shallow erosion to deposition within hollows and finally deep gully incision all in response to disturbance associated with land use change to cattle grazing. To aid this interpretation and enable estimates to be made of the magnitude of changes, pre and post European sedimentation rates were calculated for different units using the vertical distances between samples in a profile and the esti mated sample ages and uncertainty. The pre European deposition rates within Unit B at profile 5 in WPGC2 were 1.2 ± 0.14 mm yr^{-1} (Table 1: between WP 11 and 12). Whereas, post European deposition rates of Unit A ranged from 5.5 ± 0.6 mm yr^{-1} at profile 5 (Table 1: be tween WP 11 and surface) to 6.4 ± 3.1 mm yr^{-1} at profile 7 (Table 1: between WP 19 and 20), five times higher than pre European rates.

At the HBGC1 site (Figs. 2 and 13), OSL dates of gully inset floodplain deposits were <100 years old (Table 1: HB 01 to 05) and overlaid an in durated ferricrete knickpoint (Figs. 12b and 13) presumably from the Pleistocene (but not dated). Holocene deposits appear to have been either evacuated from this gully or buried and not found. Further drilling or excavation would be needed for additional dating analysis. Post European deposition rates in HBGC1 were 7.1 ± 0.65 mm yr^{-1} during the construction of the gully inset floodplain (Table 1: HB 01 to 05), which are comparable to WPGC2.

4.3. Projections of future gully growth and duration

Gully thalweg longitudinal profiles extracted from LiDAR DEM's (Fig. 12) generally displayed graded thalweg slopes over finite dis tances up to the immediate scarp zone where the profiles were

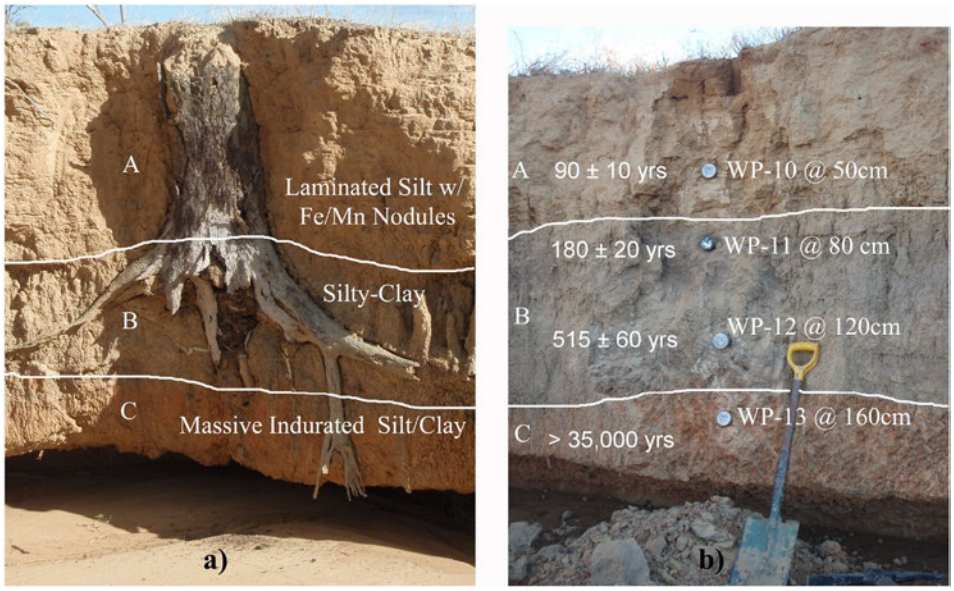

Fig. 11. Profile 5 at WPGC2b showing a) stratigraphic units and a buried tree 5 m upstream from OSL sample locations, and b) the same stratigraphic units, OSL sample locations, and measured burial ages (years BP) 5 m downstream from a).

over steepened. However for HBGC1 and KWGC2 (Fig. 12b,c), the channel profiles were interrupted by indurated ferricrete at depth. For HBGC1 (Fig. 12b), the channel slope above the indurated ferricrete knickpoint was used for profile extension because 1) the knickpoint was a permanent feature influencing the upstream channel grade and scarp retreat, and 2) the over steepened convex profile below the knickpoint was not in equilibrium due to cut and fill processes associated with both river sedimentation. For KWGC2 (Fig. 12c), the steeper channel slope below the knickpoint was used for profile extension because 1) the indurated knickpoint was actively failing and temporary, and 2) the slope of the profile below the knick point matched the channel slope a few hundred meters below the gully scarps.

Temporal estimates of when the gully scarp would reach a graded profile in all directions differed between study sites and trend projection method. The fastest observed rates of gully area expansion were at WPGC2 (Fig. 8), where linear rates projected into the future until a

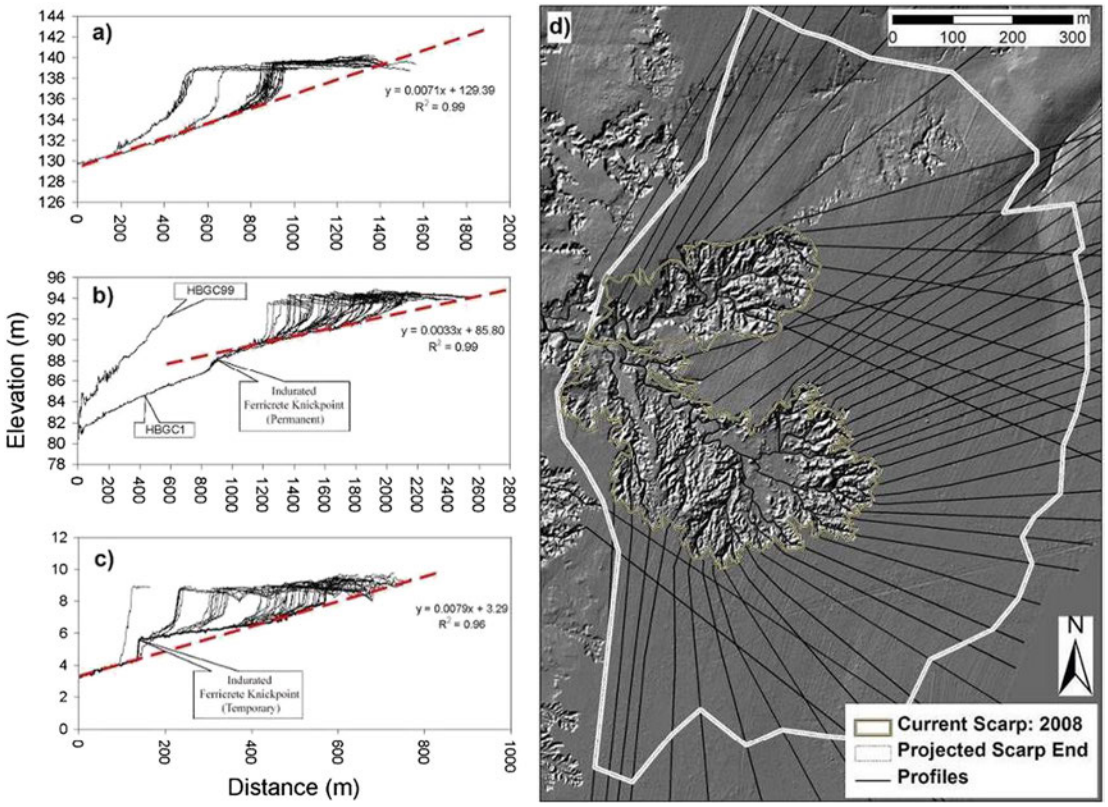

Fig. 12. Longitudinal profiles of channel thalwegs (black lines) extracted from LiDAR for a) WPGC2, b) HBGC1 and HBGC99 (bank gully), and c) KWGC2, with trend lines of thalweg slopes (dotted lines) extended beyond the scarp zone to intersection points with the river high-floodplain surface. d) WPGC2 LiDAR hillshade DEM, longitudinal profile (thalweg) extraction lines, current gully extent, and future projection of gully extent.

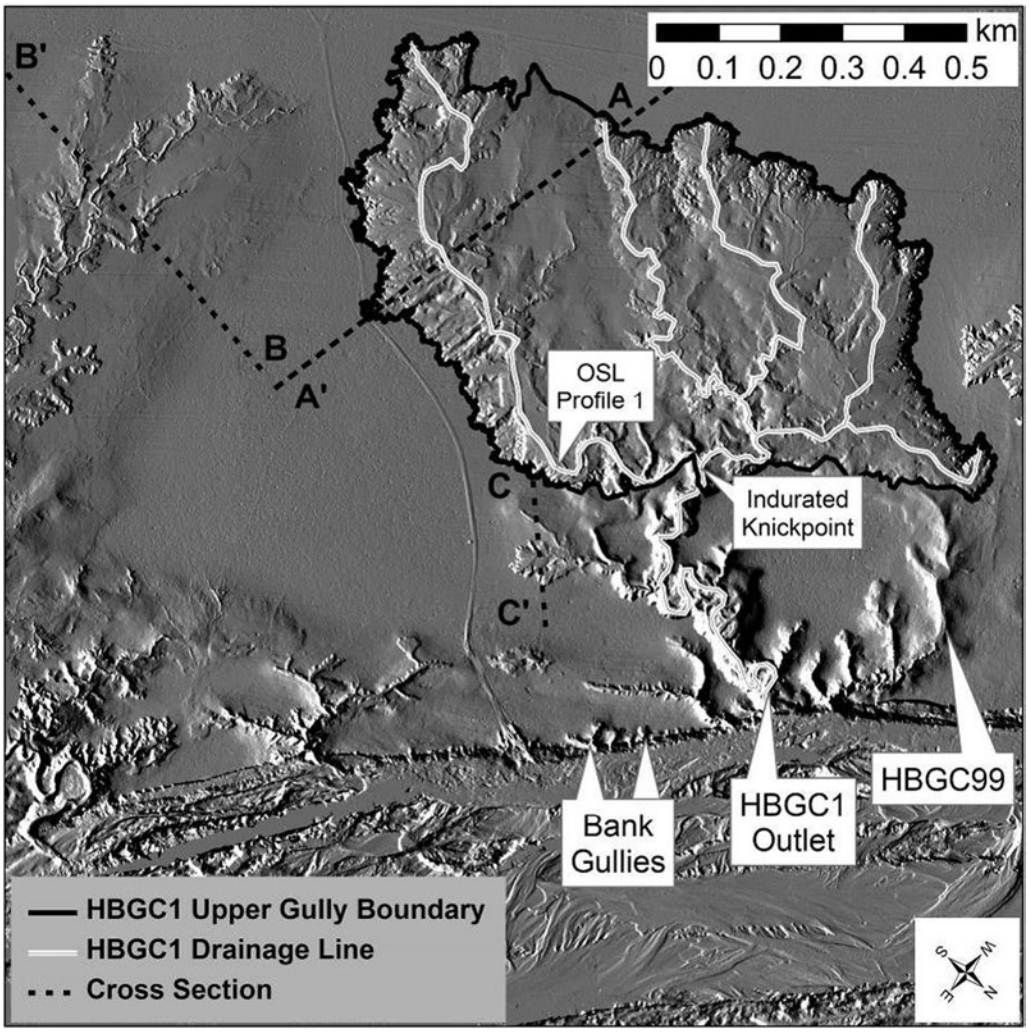

Fig. 13. LiDAR hillshade map of the left bank of the Mitchell River at HBGC1, with locations of cross-sections (Fig. 14), OSL sample location (Table 1) and the upper scarp boundary of HBGC1 above the indurated knickpoint (Fig. 12b) and main outlet channel.

graded profile was reached suggested that the gully would erode for at least another 260 years after 2010 until the year 2270, with an ultimate size 42 times its 1949 size (Fig. 12a,d). If negative exponential trends are used for projections, this changed to 290 years until a graded profile was reached. At KWGC2, both linear and negative exponential trends suggested that the gully would erode for at least another 260 years until the year 2270, to 24 times its 1958 size. In contrast, linear trends at HBGC1 projected erosion for at least ~1200 years, while negative exponential trends projected erosion for ~1700 years. The low rates of expansion at HBGC1ab ($A/A_0 < \sim 2$; Fig. 8) and the lower slope used to project profiles into the floodplain suggested that HBGC1 would only grow to 13 times its 1949 size.

4.4. Gully evolution from LiDAR data

At HBGC1 using a location for time substitution of gully form and evolution, cross sections through the main gully (A A′) were compared to several adjacent large (B B′) and small (C C′) hollows (Fig. 13). These cross sections demonstrate the transformation of uneroded shallow hollows into dissected gully complexes through lateral and vertical expansion (Fig. 14). The longitudinal profile of the main HBGC1 channel was also compared to the profile of a rounded bank gully (HBGC99) without a connection to an upslope hollow (Figs. 12b and 13). The HBGC99 bank gully profile is immi nently unstable, with head cuts starting to migrate upstream, and is much steeper compared to the HBGC1 profile that already has incised into the floodplain and upstream hollow. The incision of HBGC1 was likely contingent on its connection to the upstream hollow, while HBGC99 had its headwaters captured by the develop ment of the HBGC1 catchment. Early stages of gullying were also observed on the immediate banks of the river, where bank gullies

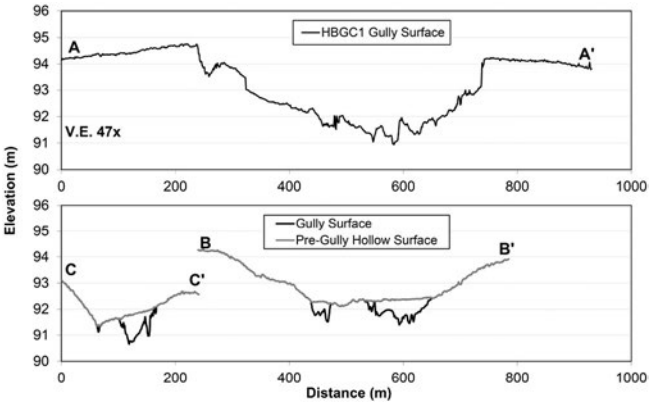

Fig. 14. Elevation cross-sections (looking downstream) from A to A′ (HBGC1), B to B′ and C to C′ in Fig. 13.

have been initiated from local disturbances (rills, stock tracks, roads, and bank erosion; Fig. 13).

5. Discussion

5.1. Gully erosion rates and area expansion

Delineating long sections of alluvial gully scarp fronts using recent GPS surveys and historical air photographs was effective for quantifying the variability in annual scarp retreat across many sites over short to medium time periods. Average linear rates of gully erosion within the Mitchell megafan (0.02 to 1.7 m yr^{-1}) were within the same order of magnitude to the most comparable study of medium term alluvial gully erosion rates (0.02 0.26 m yr^{-1}) measured by Marzolff et al. (2011) in Spain. Due to difficulty detecting subtle scarp change over short time periods due to inherent measurement error, other technologies will also be useful in measuring intra and inter annual changes at gully scarps, such as time lapse photography (Shellberg et al., 2013a), low altitude large scale aerial photographs (Marzolff et al., 2011) and/or high resolution ter restrial laser scanning (Shellberg and Brooks, 2013).

Scarp retreat rates at alluvial gullies are known to vary by time scale and measurement method (Marzolff et al., 2011; Shellberg et al., 2013b). The differences between erosion rates measured from historic air photos and recent GPS (Fig. 7) could be a result of exponential de cline in erosion rates, changes in rainfall drivers, vegetation resistance, soil erodibility and/or inherent differences in measurement methods and time scales. One half of the 18 gully sites had negative exponential trends in aerial expansion over the historical period (Fig. 8b) that would have influenced rate distributions (1949 1975 and 1975 2006; Fig. 7). Inter annual, annual and decadal rainfall totals are variable within a consistent range at these study sites and known to influence scarp re treat rates (Shellberg et al., 2013a, 2013b; Fig. 3). The drought in the 1980s could have influenced the lower rates between 1975 and 2006, but the drought was preceded and followed by wet periods in the mid 1970s and late 1990s onward. The scale and method accuracy of the scarp perimeter measurements could also be a factor. For a given gully area, the GPS method measures longer, more convoluted gully pe rimeters compared to coarser air photograph measurements. This could potentially reduce average erosion rates, but could also be offset by in creased area measurement. More detailed investigations will be needed to assess all these factors, but we do not consider these to be of signifi cance in terms of the conclusions arising out of this study.

Extrapolation of area trends back in time demonstrated that many large alluvial gully complexes were post European features (Fig. 8). Extrapolations were less certain for the slowest growing gullies, compli cated by the lack of air photo data before 1949 and uncertainty in choice of mathematical model. For all cases, it is possible that the available data over a finite period (1949 2010) might bias the trend toward a more linear form, and omit any rapid erosion rates immediately after distur bance (e.g., Graf, 1977; Simon, 1992; Rutherfurd et al., 1997).

Within supply limited colluvial gullies and hillslopes, numerous researchers have documented negative exponential decline in growth due to sediment exhaustion over time or bedrock control (Graf, 1977; Rutherfurd et al., 1997; Olley and Wasson, 2003; Rustomji and Pietsch, 2007). Other gully researchers have assumed linear trends where there was insufficient basis to determine other wise, where small sample sizes (three to four air photos) limited data exploration, or actual linear trends were present from detailed anal ysis (Shepherd, 2010; Saxton et al., 2012; Brooks et al., 2013). In this Mitchell gully study, both negative exponential trends and linear trends in area growth were observed from detailed analysis of photos each decade between 1949 and 2010, as well as the estima tion of area error margins and *RMSE*. The benefit of the negative exponential function used here is that the coefficient k can be used to explore the degree of linearity in the data, and project the time (or half life) until stabilisation. The k values (0.0007 to 0.0028) observed in these alluvial gullies were smaller than those observed or modelled in other studies (Graf, 1977; Simon, 1992; Rutherfurd et al., 1997), resulting in both near linear trends and longer relaxa tion times after disturbance, and negative exponential trends with faster initial growth and slower growth over time.

Alluvial gully erosion into dispersible floodplain soils on the Mitchell megafan is typically unconfined both horizontally and vertically (Brooks et al., 2009). Both gully elongation and lateral expansion can provide a relatively continuous supply of sediment at the transport limit, with sediment yield highly correlated to monsoonal rainfall and scarp retreat (Shellberg et al., 2013b). This can lead to near linear growth over time until grade stabilisation occurs in all directions for pe riods of several 100s to 1000s of years. However, some vertical confine ment can be provided by bedrock or indurated ferricrete layers, which could have influenced sediment availability and aerial growth rates at sites with the slowest rates and strongest exponential decline (Fig. 8b). From a long term sediment supply perspective, the fact that some alluvial gullies can potentially contribute sediment at the trans port limit (Shellberg et al., 2013b; Rose et al., 2015) is a contrast to many colluvial gullies that tend to be self limiting over timescales of a century or less (e.g. Graf, 1977; Olley and Wasson, 2003).

5.2. Gully erosion chronologies from OSL dating

Optically stimulated luminescence dating revealed that there was a major change in erosion and sedimentation patterns near and after the time of European settlement and introduction of cattle grazing (circa 1872). At WPGC2, initial shallow erosion following disturbance deposited sediment within floodplain hollows, with subsequent deep gully incision following a complex response to disturbance (sensu Schumm, 1973, 1979). While earlier forms of floodplain channel erosion and drainage hollows existed on the Mitchell floodplain during the Holocene, the rates of sedimentation post European settlement at WPGC2 were five times higher than pre European erosion rates within preceding drainage hollows. Similar gully sedimentary units, OSL dates, and post European shifts in deposition rates (0.5 mm yr^{-1} pre European; 14 mm yr^{-1} post European) have been documented in gully profiles in the adjacent Normanby River catchment (Brooks et al., 2013; Pietsch et al., 2015). These stratigraphic data define the shift from the Holocene to the Anthropocene in northern Australia (sensu Waters et al., 2016).

5.3. Projections of future gully growth and duration

The future spatial and temporal projections of gully area growth using the concept of an equilibrium grade or slope and constant average linear retreat rates represented a minimum estimate in space and time for gully scarps to stabilize. These estimates of con tinued erosion for several hundred years are reasonable from our un derstanding of alluvial gully evolution, but many uncertainties are embedded in these estimates. Actual growth trends over the next few hundred years will be influenced by non static hydro climatic and geomorphic conditions. Stabilisation could take longer if expo nential decline in growth occurs, sites are re disturbed by external forcing, and/or a reduction in sediment supply from graded scarp slopes creates sediment transport imbalances that reinitiate incision. Future climate change scenarios in northern Australia are uncertain, but increased rainfall intensity during extreme events could acceler ate erosion rates with unknown consequences. However for imme diate land management purposes, it is clear from these growth projections that alluvial gullies will remain chronic features on the landscape for at least several hundred years once initiated by natural and/or anthropogenic factors, unless erosion is mitigated by land management intervention (Shellberg and Brooks, 2013).

5.4. Gully evolution: reconciling quantitative data and explorer observations

Location for time terrain analysis using LiDAR data demonstrated that alluvial gullies can evolve from incipient gullies on channel banks into massive alluvial gully complexes (Brooks et al., 2009). At HBGC1, extrapolation of gully area trends back in time and OSL data suggested that the upper part of the dissected gully complex was not eroded in 1845 when Leichhardt and Gilbert passed this location. However, both journal records (Gilbert, 1845; Leichhardt, 1847) and LiDAR data indi cate that rounded fluvial features (floodplain hollows and precursor gullies on steep river banks) were likely present in 1845 which would have been exhausting to repetitively ride horses through. It is deduced that incipiently unstable bank gullies, adjacent floodplain hollows, and other inherited (antecedent) features co evolved and incised into the massive gully complexes during the post European period. The initia tion of gullying into river banks, precursor gullies, and floodplain hollows was dependent on natural and anthropogenic disturbance factors that triggered incision into these unstable features.

5.5. Sediment production from alluvial gullies across the megafan

The erosion rate data presented here can be used to update earlier estimates of sediment production from alluvial gullies in the Mitchell catchment (Brooks et al., 2008, 2009; Rustomji et al., 2010). These cal culations are based on recent and historic median rates of annual scarp retreat, catchment gully distribution, gully scarp perimeter mea surements, scarp heights correlated to relative relief and downriver floodplain elevation, and soil bulk densities. It is now estimated that ~6.3 Mt yr^{-1} of sand, silt, and clay were eroded historically (1949 2006) from alluvial gullies, compared to ~3.9 Mt yr^{-1} recently (2005 2010). There is still uncertainty in these data due to the spatial and temporal variability in scarp retreat rates and the accuracy of map ping the density of all alluvial gullies at the landscape scale (Brooks et al., 2008, 2009; Shellberg et al., 2013a, 2013b). However, compared to other components of the Mitchell catchment sediment budget or sed iment yield estimates at downstream gauges (Brooks et al., 2008; Rustomji et al., 2010; Shellberg, 2011; Shellberg et al., 2013b), these alluvial gullies are a major component of the sediment budget. Inde pendent sediment tracing research in the Mitchell catchment has confirmed that sub surface soils from gully erosion, channel erosion, deep rilling and scalded soils dominate the fine sediment budget (Caitcheon et al., 2012).

5.6. Gully initiation and geomorphic thresholds

Understanding the possible mechanisms that contributed to the ac celeration of gully initiation and erosion following European settlement requires a process based analysis of geomorphic change, which is pro vided here. The initiation of gully erosion and channel incision is influ enced by internal and external factors that can exceed geomorphic thresholds resulting in instability and landform change (e.g., Schumm and Hadley, 1957; Schumm, 1973, 1979; Cooke and Reeves, 1976; Graf, 1979; Prosser et al., 1994; Prosser and Slade, 1994; Tucker et al., 2006). Long term factors include climate, geology, soil type, weathering, relief, base level, slope angles, sediment storage volume, and inherited or antecedent terrain. Factors influential over shorter time periods include fluctuations in rainfall and hydrology, changes in vegetation cover and resistance, and anthropogenic land use (Schumm and Lichty, 1965; Phillips, 2010).

The over steepened bank slopes along channels of the upper Mitchell megafan are a result of fan head trenching since the late Pleistocene (Grimes and Doutch, 1978; Fig. 1). This incision could have been influenced by changes in base level (Chappell et al., 1982; Nanson et al., 2013), reductions in sediment supply in the Ho locene after a major period of floodplain and fan sedimentation during the Last Glacial Maximum (Nanson et al., 1992; Thomas et al., 2001), and changes to rainfall and water runoff as the current monsoonal climate regime developed (Kershaw, 1978; Kershaw and Nanson, 1993). The reduced connectivity of flood water with the megafan surface after incision (Shellberg et al., 2013a) trans formed the high floodplain from an aggrading to a degrading envi ronment. Incision and tropical weathering through the Holocene made available large volumes of dispersible sodic soils (Isbell et al., 1968; Galloway et al., 1970; Biggs and Philip, 1995). The potential for alluvial gully erosion increased where the local relative relief and bank slope was greatest and coincident with these highly dis persible soils (Brooks et al., 2009; Shellberg et al., 2013a).

The inherited (antecedent) floodplain terrain adjacent to river chan nels on the Mitchell megafan influenced the potential for gully initiation and propagation. These inherited features include shallow flood drain age hollows, steep rounded gullies on immediate river banks, fluvial levees, paleo channels and lagoons, and larger creeks. Their spatial dis tribution is highly contingent on the local evolution of the floodplain or megafan surface (e.g., Wilkinson et al., 2006; Phillips and Slattery, 2008). While inherited floodplain features are not requisite for gully ini tiation or expansion (Brooks et al., 2009), they can be especially unsta ble components of the landscape. These topographic irregularities are preferential locations for surface or soil water draining off the flood plain, often have unique soil conditions, are preferential cattle grazing areas or migration routes, and thus are inherently prone to degradation by gully incision.

The monsoonal climate of the Cape York Peninsula has been relative ly stable over the last 6000 years following the Last Glacial Maximum compared to longer term glacial interglacial cycles (Kershaw, 1978; Kershaw and Nanson, 1993). However, decadal fluctuations in climate due to ENSO cycles (Lough, 1991; Risbey et al., 2009; Fig. 3) are a signa ture of the current climate, with additional variability in the occurrence of tropical cyclones. In the Mitchell catchment, Nott et al. (2007) mea sured oxygen isotope ratios in limestone stalagmites as a rainfall proxy and documented that cyclone landing frequency and magnitude were relatively high from CE 1400 and 1800, and comparatively low from CE 1800 2000 during the period when a majority of these alluvial gullies initiated. The floodplain sediment into which these alluvial gullies are eroding has an age >35,000 years BP, and has persisted most ly intact through the Holocene despite river and major tributary inci sion. Therefore, while climate variability is no doubt important, it is not a new phenomenon, and cannot alone explain the recent synchro nous incision and acceleration of alluvial gullying across the Mitchell megafan (this study), the neighbouring Normanby catchment (Brooks et al., 2013; Shellberg and Brooks, 2013) and other floodplains across northern Australia (Condon, 1986; McCloskey, 2010) during the last 100 years of European settlement and land use.

The kinetic energy from rainfall, in channel and overbank river dis charge, and floodplain drainage is the main driver for alluvial gully erosion initiation and propagation. Monsoonal convective storms in the Mitchell catchment have moderately high rainfall intensity and erosivity that dominate rill initiation and gully erosion processes (Shellberg et al., 2013a). Wet and dry cycles at the storm, annual, and decadal scale can influence the kinetic energy available for erosion (Lough, 1991; Nott et al., 2007; Risbey et al., 2009; Shellberg et al., 2013a). Extreme rainfall events, such as from tropical cyclones (Nott et al., 2007), can lead to large scale flooding along rivers that can also play a role in alluvial gully initiation and propagation. River backwater and overbank flooding into floodplain hollows was observed to increase gully erosion at KWGC2 (Shellberg et al., 2013a), but this is not a prerequisite for gully activity; rather it can add to ubiquitous rainfall driven erosion. Scour of floodplain drainage channels can occur during flood drawdown, as can failure and slumping of river banks from scour and water seepage. Bank erosion is widespread along the lower Mitchell River (Brooks et al., 2008). Linear bank retreat could initiate 'continuous scarp front' gullies (Brooks et al., 2009), as well as destabilize adjacent floodplain drainage channels.

The stability of valley floors and initiation of gullying depends on the balance between the critical shear stress of flowing water needed to entrain sediment and the resisting and energy dissipating factors of vegetative cover. Reduced vegetative cover or biomass for a given hydrological regime can induce channel incision and gullying (Graf, 1979; Prosser and Slade, 1994). Both natural factors (such as drought and fire) and anthropogenic land use can influence vegetative cover and thresholds of gully erosion. The initiation of gully erosion corresponding with vegetation disturbance after the introduction of cattle has been observed on other alluvial plains and valleys in Australia (e.g., Eyles, 1977; Condon, 1986; Pickup, 1991; Prosser and Winchester, 1996; Pringle et al., 2006).

Major land use change from traditional Aboriginal management to cattle grazing (Fig. 4) undoubtedly disturbed the soil and native grass of riparian woodlands across the Mitchell megafan. Mismanagement of cattle and the landscape was widespread (QSA, 2008; Shellberg, 2011), as described for the Wrotham Park Aggregation: "*no property in the North has been maintained or cared for worse, and this includes the quality of cattle and horses, together with plant and improvements*" (W. Reid, Queensland Primary Producers Co op, 3rd Dec 1963; QSA, 2008).

Along the Mitchell River, cattle congregated in riparian zones for water access and grass feed from fertile soils, and were concentrated along river stock routes during cattle drives (QSA, 2008). Grazing, and soil disturbance by cattle hoofs, reduced native perennial grass cover and vigour that were essential for stabilizing dispersible soils (Shellberg and Brooks, 2013). Soil disturbance and the reduction of soil organic cover promoted the scalding of sodic soils, loss of biological crusts, soil compaction, reduced infiltration, and accelerated water runoff, as observed in other tropical rangelands (e.g., Bridge et al., 1983; McIvor et al., 1995; Dunne et al., 2011). Dense and deep cattle tracks (pads) traversed steep banks down to water holes, cut into the fragile soils, and channelled overland flow from rainfall and floodwater into gullies (e.g., Condon, 1986; Brooks et al., 2009; Shellberg and Brooks, 2013). Cattle tracks also followed the easiest path to water; in many cases this was down incipiently unstable floodplain hollows and rounded bank gullies. Weed invasion into riparian zones became commonplace by the 1920s (QSA, 2008; Shellberg, 2011). Major changes to the fire regime also occurred, with a shift from low intensity early dry season fires and mosaic burning by Aboriginal people, toward greater fire suppression by pastoralists with limited use of fire in the early dry and early wet seasons to control cattle and maximize feed, but not maintain grass cover or vigour (Hann, 1872; Crowley and Garnett, 2000).

The initiation and propagation of alluvial gullies across the Mitchell megafan were undoubtedly influenced by multiple synergistic factors. The long term evolution of the Mitchell megafan and inherited floodplain features provided the inherent gully erosion potential, while shorter term hydroclimatic drivers and land use impacts on vegetative cover and soil erosion resistance helped push the landscape across a stability threshold. For example, the rapid increase of cattle in the lower Mitchell after 1900 (Fig. 4) was coincident with several years of above average rainfall (Fig. 3). Cattle numbers remained relatively high into the subsequent dry phase in the late 1910s, both of which likely reduced grass cover and increased the effective kinetic energy of rainfall impacting soil. These natural climate variations could have exacerbated the erosional impacts of cattle that were not destocked from sensitive areas during long dry seasons and drought years, similar to elsewhere in Australia (McKeon et al., 2004; Stafford Smith et al., 2007).

6. Conclusions

Along the Mitchell fluvial megafan, historic trends in alluvial gully area extrapolated back in time suggested that most large alluvial gully complexes are post European features. OSL dating quantified an increase in gully deposition rates after the introduction of cattle grazing and land use change, following a complex response of initial soil stripping, deposition in hollows, and then deep gully incision. LiDAR terrain analysis, OSL data, and air photos suggested that incipiently unstable bank gullies and floodplain hollows observed by European explorers subsequently coevolved and incised into sediments deposited >35,000 BP to become the massive gully complexes observable today. While uncertainty remains in defining the exact processes and mechanisms for triggering gully initiation, both natural (extreme rainfall, floods, and drought) and anthropogenic (grazing, fire, weeds, and roads) disturbance factors likely worked synergistically to erode unstable landscape features. Once initiated, these gullies will continue to erode large areas of riparian landscape for hundreds if not thousands of years.

This study has obvious implications for improving land management across northern Australia and beyond. A major paradigm shift in grazing land management has long been needed (e.g., Winter, 1990), in order to maintain native grass health and cover, reduce soil disturbance and erosion, re introduce sustainable fire regimes, reduce exotic and woody weed invasion, and adjust to climate variability (Stafford Smith et al., 2007). Improved land management would see cattle excluded or spelled from riparian zones and steep banks and associated hollows across wide areas of river frontage (>4 km, Brooks et al., 2009) via fencing, off stream water point development, and/or sustainable grazing rates on stable soils away from river frontage. This will reduce the initiation of new alluvial gullies, slow gully erosion rates where already initiated, and aid in passive or proactive gully rehabilitation efforts (Shellberg and Brooks, 2013).

This study demonstrates the vulnerability of floodplains and megafans to gully erosion. The nature and extent of alluvial gullying should be investigated in more detail on other floodplains and megafans globally, as well as their sensitivity to degradation from intrinsic and extrinsic variables, land use change, and future climate change. Our understanding of floodplains and megafans as predominantly depositional environments needs to change to incorporate deposition and erosion cell dynamics over a variety of spatial and temporal scales along the (dis)continuum of process domains, channel evolution, and antecedent alluvial morphology.

Acknowledgements

The Tropical Rivers and Coastal Knowledge (TRaCK) program, Caring for Our Country program, Northern Gulf NRM Group, Land and Water Australia, and Griffith University funded this project. Terry Culpitt and staff at the Queensland Department of Environment and Resource Management provided historic air photograph support. Jorg Hacker and Wolfgang Lieff from Airborne Research Australia acquired and processed the airborne LiDAR data. Ken McMillan and Chris Leslie at CSIRO and Daniel Borombovits and Jon Olley at Griffith University provided OSL support and advice. Field assistance was provided by the Kowanyama Rangers, Kris Jaeger, Garrett Bean and Ariane Hefferan. Project support was provided by Deb Eastop, Brynn Mathews and Bill Sokolich at the Mitchell River Watershed Management Group, and Noeline Ikin and Tim Hoogwerf at the Northern Gulf Resource Management Group. Cultural guidance by Aboriginal Traditional Owners was provided by the late Vivian Lane for Gugu Mini country and by Willie Banjo and the Kowanyama Rangers for Yir Yoront country. We especially thank the managers of Wrotham Park, Highbury and Dunbar Stations and the Kowanyama Aboriginal Land Office for property access and the time to discuss the management, challenges, and beauty of the lower Mitchell catchment. Critical but constructive reviews by Justin Wilkinson and several anonymous reviewers improved the manuscript.

References

ABOM (Australian Bureau of Meteorology), 2015. Climate data. Accessed online in 2015 at: http://www.bom.gov.au/climate/.

ABS (Australian Bureau of Statistics), 2008. 7124.0- Historical Selected Agriculture Commodities, by State (1861 to Present), Total Cattle Numbers. Australian Bureau of Statistics.

Aitken, M.J., 1998. Introduction to Optical Dating: Dating of Quaternary Sediments by the Use of Photon-Stimulated Luminescence. Clarendon Press (280 pp.).
Arnold, G., 1997. Grazier experience with Stylosanthes technology. III. Wrotham Park, 1963–1988. Trop. Grasslands 31, 522–526.
Arnold, L.J., Roberts, R.G., Galbraith, R.F., DeLong, S.B., 2009. A revised burial dose estimation procedure for optical dating of young and modern-age sediments. Quat. Geochronol. 4, 306–325.
Bartley, R., Hawdon, A., Post, D.A., Roth, C.H., 2007. A sediment budget for a grazed semi-arid catchment in the Burdekin basin, Australia. Geomorphology 87, 302–321.
Bartley, R., Wilkinson, S.N., Hawdon, A.A., Abbott, B.N., Post, D.A., 2010. Impacts of improved grazing land management on sediment yields part 2: catchment response. J. Hydrol. 389, 249–259.
Biggs, A.J.W., Philip, S.R., 1995. Soils of Cape York Peninsula. Queensland Department of Primary Industries. Mareeba, Qld.
Bowman, D.M.J.S., Sharp, B.R., Zoppi, U., 2004. Isotopic (^{13}C and ^{14}C) evidence supporting the transformative effect of cattle on north Australian vegetation. J. Biogeogr. 31, 1373–1375.
Bridge, B.J., Mott, J.J., Hartigan, R.J., 1983. The formation of degraded areas in the dry savanna woodlands of Northern Australia. Aust. J. Soil Res. 21, 91–104.
Brooks, A.P., Brierley, G.J., 1997. Geomorphic responses of lower Bega River to catchment disturbance, 1851–1926. Geomorphology 18, 291–304.
Brooks, A.P., Spencer, J., Shellberg, J.G., Knight, J., Lymburner, L., 2008. Using Remote Sensing to Quantify Sediment Budget Components in a Large Tropical River — Mitchell River, Gulf of Carpentaria. *Sediment Dynamics in Changing Environments* (Proceedings of a Symposium Held in Christchurch, New Zealand, December 2008). IAHS Publ. 325, pp. 225–236.
Brooks, A.P., Shellberg, J.G., Spencer, J., Knight, J., 2009. Alluvial gully erosion: an example from the Mitchell fluvial megafan, Queensland, Australia. Earth Surf. Process. Landf. 34, 1951–1969 (With 2010 Erratum, Earth Surf. Process. Landf., 35, 242–245).
Brooks, A., Spencer, J., Olley, J., Pietsch, T., Borombovits, D., Curwen, G., Shellberg, J., Howley, C., Gleeson, A., Simon, A., Bankhead, N., Klimetz, D., Eslami-Endargoli, L., Bourgeault, A., 2013. An Empirically-Based Sediment Budget for the Normanby Basin: Sediment Sources, Sinks, and Drivers on the Cape York Savannah. Final Report for the Australian Government Caring for our Country — Reef Rescue Program. Griffith University, Australian Rivers Institute (Available at: http://www.capeyorkwaterquality.info/downloads).
Caitcheon, G.C., Olley, J.M., Pantus, F., Hancock, G., Leslie, C., 2012. The dominant erosion processes supplying fine sediment to three major rivers in tropical Australia, the Daly (NT), Mitchell (Qld) and Flinders (Qld) Rivers. Geomorphology 151-152, 188–195.
Chappell, J., Rhodes, E.G., Thom, B.G., Wolanski, E., 1982. Hydro-isostasy and the sea-level isobase of 5500 BP in North Queensland, Australia. Mar. Geol. 49 (1–2), 81–90.
Chivas, A.R., Garcia, A., van der Kaars, S., Couapel, M.J.J., Holt, S., Reeves, J.M., Wheeler, D.J., Switzer, A.D., Murray-Wallace, C.V., Banerjee, D., Price, D.M., Wang, S.X., Pearson, G., Edgar, N.T., Beaufort, L., De Deckker, P., Lawson, E., Cecil, C.B., 2001. Sea-level and environmental changes since the last interglacial in the Gulf of Carpentaria, Australia: an overview. Quat. Int. 83-5, 19–46.
Condon, R.W., 1986. A Reconnaissance Erosion Survey of Part of the Victoria River District, N.T. Hassall and Associates, Canberra.
Condon, R.W., Newman, J.C., Cunningham, G.M., 1969. Soil erosion and pasture degeneration in Central Australia: part 1 — soil erosion and degeneration of pastures and topfeeds. J. Soil Conserv. Serv. NSW 25, 47–92.
Cooke, R.U., Reeves, R., 1976. Arroyos and Environmental Change in the American South-West. Clarendon Press, London.
Crowley, G.M., Garnett, S.T., 1998. Vegetation change in the grasslands and grassy woodlands of east-central Cape York Peninsula, Australia. Pac. Conserv. Biol. 4 (2), 132–148.
Crowley, G.M., Garnett, S.T., 2000. Changing fire management in the pastoral lands of Cape York Peninsula of Northeast Australia, 1623 to 1996. Aust. Geogr. Stud. 38 (1), 10–26.
Dunne, T., Western, D., Dietrich, W.E., 2011. Effects of cattle trampling on vegetation, infiltration, and erosion in a tropical rangeland. J. Arid Environ. 75 (1), 58–69.
Edye, L.A., Gillard, P., 1985. Pasture Improvement in Semi-Arid Tropical Savannas: A Practical Example in Northern Queensland. In: Tothill, J.C., Mott, J.J. (Eds.), Ecology and Management of the World's Savannas. Australian Academy of Science, Canberra, ACT, pp. 303–309.
Eyles, R.J., 1977. Changes in drainage networks since 1820, Southern Tablelands, N.S.W. Aust. Geogr. 13, 377–386.
Fanning, P.C., 1999. Recent landscape history in arid western New South Wales, Australia: a model for regional change. Geomorphology 29 (3–4), 191–209.
Fensham, R.J., Skull, S.D., 1999. Before cattle: a comparative floristic study of eucalyptus savanna grazed by macropods and cattle in north Queensland, Australia. Biotropica 31 (1), 37–47.
Galbraith, R.F., Roberts, R.G., 2012. Statistical aspects of equivalent dose and error calculation and display in OSL dating: an overview and some recommendations. Quat. Geochronol. 11, 1–27.
Galloway, R.W., Gunn, R.H., Story, R., 1970. Lands of the Mitchell-Normanby Area, Queensland. CSIRO, Land Research Series 26, pp. 1–101.
Gilbert, J., 1845. Diary of the Port Essington Expedition, 18 Sept. 1844–28 June 1845. Mitchell Library: State Library of New South Wales (226 pp.).
Graf, W.L., 1977. The rate law in fluvial geomorphology. Am. J. Sci. 277, 178–191.
Graf, W.L., 1979. The development of montane arroyos and gullies. Earth Surf. Process. 4, 1–14.
Grimes, K.G., Doutch, H.F., 1978. The late Cainozoic evolution of the Carpentaria Plains, Northern Queensland. BMR J. Aust. Geol. Geophys. 3, 101–112.
Hancock, G.R., Evans, K.G., 2010. Gully, channel and hillslope erosion – an assessment for a traditionally managed catchment. Earth Surf. Process. Landf. 35, 1468–1479.
Hancock, G.J., Wilkinson, S.N., Hawdon, A.A., Keen, R.J., 2014. Use of fallout tracers 7Be, 210Pb and 137Cs to distinguish the form of sub-surface soil erosion delivering sediment to rivers in large catchments. Hydrol. Process. 28 (12), 3855–3874.
Hann, W., 1872. Expedition of Exploration to the Endeavour River, Cape York Peninsula, 1872. Reconstructed from his Diary and two Notebooks by Harry Clarke, 1982, with an Introduction by Helen Mays (81 pp.).
Hughes, M.L., McDowell, P.F., Marcus, W.A., 2006. Accuracy assessment of georectified aerial photographs: implications for measuring lateral channel movement in a GIS. Geomorphology 74, 1–16.
Hughes, A., Olley, J.M., Croke, J., Webster, I., 2009. Determining floodplain sedimentation rates using 137Cs in a low fallout environment dominated by channel- and cultivation-derived sediment inputs, central Queensland. Aust. J. Environ. Radioact. 100, 858–886.
Isbell, R.F., Webb, A.A., Murtha, G.G., 1968. Atlas of Australian Soils - Explanatory Data for Sheet 7 North Queensland. CSIRO and Melbourne University Press, Victoria.
Jardine, F., Jardine, A., 1867. Narrative of the Overland Expedition of the Messrs. Jardine, from Rockhampton to Cape York, Northern Queensland, 1864–1865. In: Byerley, Frederick J. (Ed.), Compiled from the Journals of the Brothers. J.W. Buxton Publisher, Brisbane (engineer of roads, northern division of Queensland). (Available at www.gutenberg.net).
Jones, D.A., Wang, W., Fawcett, R., 2009. High-quality spatial climate data-sets for Australia. Aust. Meteorol. Oceanogr. J. 58, 233–248.
Kershaw, A.P., 1978. Record of last interglacial cycle from northeast Queensland. Nature 272, 159–161.
Kershaw, A.P., Nanson, G.C., 1993. The last full glacial cycle in the Australian region. Glob. Planet. Chang. 7, 1–9.
Lal, R., 1992. Restoring land degraded by gully erosion in the tropics. Adv. Soil Sci. 17, 123–151.
Lane, E.W., 1955. Design of stable channels. Trans. Am. Soc. Civ. Eng. 120, 1234–1279.
Leichhardt, L., 1847. Journal of an Overland Expedition in Australia: From Moreton Bay to Port Essington, a Distance of Upwards of 3000 miles, During the Years 1844–1845. T&W Boone, London (544 pp.).
Lough, J.M., 1991. Rainfall variations in Queensland, Australia: 1891–1986. Int. J. Climatol. 11 (7), 745–768.
Mackin, J.H., 1948. Concept of the graded river. Geol. Soc. Am. Bull. 59, 463–512.
Marzolff, I., Ries, J.B., Poesen, J., 2011. Short-term versus medium-term monitoring for detecting gully-erosion variability in a Mediterranean environment. Earth Surf. Process. Landf. 36 (12), 1604–1623.
McCloskey, G.L., 2010. Riparian Erosion Morphology, Processes and Causes along the Victoria River, Northern Territory, Australia. Charles Darwin University, p. 200 (PhD Thesis).
McIvor, J.G., Williams, J., Gardener, C.J., 1995. Pasture management influences runoff and soil movement in the semi-arid tropics. Aust. J. Exp. Agric. 35, 55–65.
McKeon, G., Hall, W., Henry, B., Stone, G., Watson, I., 2004. Pasture Degradation and Recovery in Australia's Rangelands: Learning from History. Queensland Dept. of Natural Resources, Mines and Energy, Indooroopilly, Qld. (256 pp.).
Medcalff, F.G., 1944. Soil Erosion Reconnaissance of the Ord River Valley and Watershed. Report to the Department of Lands and Surveys, Western Australia.
Mejdahl, V., 1979. Thermoluminescence dating: beta-dose attenuation in quartz grains. Archaeometry 21 (1), 61–72.
Mertes, L.A.K., Dunne, T., 2008. Effects of Tectonism, Climate Change, and Sea-Level Change on the Form and Behaviour of the Modern Amazon River and its Floodplain. In: Gupta, A. (Ed.), Large Rivers: Geomorphology and Management. John Wiley and Sons, West Sussex, UK, pp. 115–144.
Murray, A.S., Marten, R., Johnston, A., Martin, P., 1987. Analysis for naturally occurring radionuclides at environmental concentrations by gamma spectrometry. J. Radioanal. Nucl. Chem. Artic. 115 (2), 263–288.
Nanson, G.C., Price, D.M., Short, S.A., 1992. Wetting and drying of Australia over the past 300 ka. Geology 20, 791–794.
Nanson, R.A., Vakarelov, B.K., Ainsworth, R.B., Williams, F.M., Price, D.M., 2013. Evolution of a Holocene, mixed-process, forced regressive shoreline: the Mitchell River delta, Queensland, Australia. Mar. Geol. 339, 22–43.
Neldner, V.J., Stanton, J.P., Fensham, R.J., Clarkson, J.R., 1997. The natural grasslands of Cape York Peninsula, Australia. Description, distribution and conservation status. Biol. Conserv. 81 (1–2), 121–136.
Nott, J., Haig, J., Neil, H., Gillieson, D., 2007. Greater frequency variability of landfalling tropical cyclones at centennial compared to seasonal and decadal scales. Earth Planet. Sci. Lett. 255 (3–4), 367–372.
Olley, J.M., Wasson, R.J., 2003. Changes in the flux of sediment in the Upper Murrumbidgee catchment, Southeastern Australia, since European settlement. Hydrol. Process. 17 (16), 3307–3320.
Olley, J.M., Pietsch, T., Roberts, R.G., 2004. Optical dating of Holocene sediments from a variety of geomorphic setting using single grains of quartz. Geomorphology 60, 337–358.
Olley, J., Brooks, A., Spencer, J., Pietsch, T., Borombovits, D., 2013. Subsoil erosion dominates the supply of fine sediment to rivers draining into Princess Charlotte Bay, Australia. J. Environ. Radioact. 124, 121–129.
Parker, G., Muto, T., Akamatsu, Y., Dietrich, W.E., Lauer, J.W., 2008. Unravelling the conundrum of river response to rising sea-level from laboratory to field. Part II. The Fly–Strickland River system, Papua New Guinea. Sedimentology 55, 1657–1686.
Payne, A.L., Kubicki, A., Wilcox, D.G., Short, L.C., 1979. A Report on the Erosion and Range Condition in the West Kimberley Area of Western Australia. Technical Bulletin No. 42. Department of Agriculture of Western Australia, p. 52.
Phillips, J.D., 2010. Relative importance of intrinsic, extrinsic, and anthropic factors in the geomorphic zonation of the Trinity River, Texas. J. Am. Water Resour. Assoc. 46 (4), 807–823.

Phillips, J.D., Slattery, M.C., 2008. Antecedent alluvial morphology and sea level controls on form-process transition zones in the lower Trinity River, Texas. River Res. Appl. 24, 293–309.
Pickup, G., 1985. The erosion cell: a geomorphic approach to landscape classification in range assessment. Aust. Rangel. J. 7 (2), 114–121.
Pickup, G., 1991. Event frequency and landscape stability on the floodplain systems of arid Central Australia. Quat. Sci. Rev. 10, 463–473.
Pietsch, T.J., 2009. Optically stimulated luminescence dating of young (<500 years old) sediments: testing estimates of burial dose. Quat. Geochronol. 4 (5), 406–422.
Pietsch, T.J., Brooks, A.P., Spencer, J., Olley, J.M., Borombovits, D., 2015. Age, distribution, and significance within a sediment budget, of in-channel depositional surfaces in the Normanby River, Queensland, Australia. Geomorphology 239, 17–40.
Poesen, J., Valentin, C., Nachtergaele, J., Verstraeten, G., 2003. Gully erosion and environmental change: importance and research needs. Catena 50 (2–4), 91–133.
Pringle, H.J.R., Watson, I.W., Tinley, K.L., 2006. Landscape improvement, or ongoing degradation reconciling apparent contradictions from the arid rangelands of Western Australia. Landsc. Ecol. 21 (8), 1267–1279.
Prosser, I.P., Slade, C.J., 1994. Gully formation and the role of valley-floor vegetation, Southeastern Australia. Geology 22 (12), 1127–1130.
Prosser, I.P., Winchester, S.J., 1996. History and processes of gully initiation and development in eastern Australia. Z. Geomorphol. Suppl. Bnd. 105, 91–109.
Prosser, I.P., Chappell, J., Gillespie, R., 1994. Holocene valley aggradation and gully erosion in headwater catchments, south-eastern highlands of Australia. Earth Surf. Process. Landf. 19, 465–480.
QSA (Queensland State Archives), 2008. Pastoral run files for Wrotham Park, Gamboola, Gamboola South, Highbury, and Drumduff cattle stations. Accessed in 2008 in Runcorn Queensland: http://www.archivessearch.qld.gov.au.
Risbey, J.S., Pook, M.J., McIntosh, P.C., Wheeler, M.C., Hendon, H.H., 2009. On the remote drivers of rainfall variability in Australia. Mon. Weather Rev. 137, 3233–3253.
Rose, C.W., Shellberg, J.G., Brooks, A.P., 2015. Modelling suspended sediment concentration and load in a transport-limited alluvial gully in northern Queensland, Australia. Earth Surf. Process. Landf. 40 (10), 1291–1303.
Rustomji, P., Pietsch, T., 2007. Alluvial sedimentation rates from southeastern Australia indicate post-European settlement landscape recovery. Geomorphology 90, 73–90.
Rustomji, P., Shellberg, J., Brooks, A., Spencer, J., Caitcheon, G., 2010. A Catchment Sediment and Nutrient Budget for The Mitchell River, Queensland. A Report to the Tropical Rivers and Coastal Knowledge (TRaCK) Research Program. CSIRO Water for a Healthy Country National Research Flagship (119 pp., Available at: http://track.gov.au/publications/registry/876).
Rutherfurd, I.D., Prosser, I.P., Davis, J., 1997. Simple Approaches to Predicting Rates and Extent of gully Development. In: Wang, S.S.Y., Langendoen, E.J., Shields, F.D.J. (Eds.), Proceedings of the Conference on Management of Landscapes Disturbed by Channel Incision. The Centre for Computational Hydroscience and engineering. The University of Mississippi, pp. 1124–1130.
Sattar, F., 2011. Geoinformatics Based Framework for Three Dimensional Gully Mapping and Erosion Volume Calculation (PhD Dissertation) School of Environment and Life Sciences, Charles Darwin University, Australia (191 pp.).
Saxton, N.E., Olley, J.M., Smith, S., Ward, D.P., Rose, C.W., 2012. Gully erosion in subtropical south-east Queensland, Australia. Geomorphology 173-174, 80–87.
Schumm, S.A., 1973. Geomorphic Thresholds and Complex Response of Drainage Systems. In: Morisawa, M. (Ed.), Fluvial Geomorphology. Allen and Unwin, London, pp. 299–310.
Schumm, S.A., 1977. The Fluvial System. Wiley, New York.
Schumm, S.A., 1979. Geomorphic thresholds: the concept and its applications. Trans. Inst. Br. Geogr. 4, 485–515.
Schumm, S.A., Hadley, R.F., 1957. Arroyos and the semiarid cycle of erosion. Am. J. Sci. 255, 161–174.
Schumm, S.A., Lichty, R.W., 1965. Space, time and causality in geomorphology. Am. J. Sci. 263, 110–119.
Sharp, R.L., 1934. The Social Organisation of the Yir Yoront Tribe, Cape York Peninsula (PhD Dissertation) Harvard University.
Sharp, B.R., Bowman, D.M.J.S., 2004. Net woody vegetation increase confined to seasonally inundated lowlands in an Australian tropical savanna, Victoria River District, Northern Territory. Austral Ecol. 29, 667–683.
Sharp, B.R., Whittaker, R.J., 2003. The irreversible cattle-driven transformation of a seasonally flooded Australian savanna. J. Biogeogr. 30, 783–802.
Shellberg, J.G., 2011. Alluvial Gully Erosion Rates and Processes across the Mitchell River Fluvial Megafan in Northern Queensland, Australia (PhD Dissertation) Griffith University, Brisbane, Australia (248 pp.).
Shellberg, J.G., Brooks, A.P., 2013. Alluvial Gully Prevention and Rehabilitation Options for Reducing Sediment Loads in the Normanby Catchment and Northern Australia. Final Report for the Australian Government's Caring for our Country - Reef Rescue Initiative. Griffith University, Australian Rivers Institute (312 pp., http://www.capeyorkwaterquality.info/references/cywq-223).
Shellberg, J.G., Brooks, A.P., Spencer, J., Ward, D., 2013a. The hydrogeomorphic influences on alluvial gully erosion along the Mitchell River fluvial megafan, northern Australia. Hydrol. Process. 27 (7), 1086–1104.
Shellberg, J.G., Brooks, A.P., Rose, C.W., 2013b. Sediment production and yield from an alluvial gully in northern Queensland, Australia. Earth Surf. Process. Landf. 38, 1765–1778.
Shepherd, R., 2010. Changes in gully Erosion along the Upper Burdekin River Frontage in North Queensland. In: Eldridge, D.J., Waters, C. (Eds.), Proceedings of the 16th Biennial Conference of the Australian Rangeland Society. Australian Rangeland Society, Perth.
Simon, A., 1992. Energy, time and channel evolution in catastrophically disturbed fluvial systems. Geomorphology 5, 345–372.
Simpson, C.J., Doutch, H.F., 1977. The 1974 wet-season flooding of the southern Carpentaria Plains, northwest Queensland. BMR J. Aust. Geol. Geophys. 2, 43–51.
Stafford Smith, D.M., McKeon, G.M., Watson, I.W., Henry, B.K., Stone, G.S., Hall, W.B., Howden, S.M., 2007. Learning from episodes of degradation and recovery in variable Australian rangelands. Proc. Natl. Acad. Sci. U. S. A. 104 (52), 20691.
Stokes, S., Ingram, S., Aitken, M.J., Sirocko, F., Anderson, R., Leuschner, D., 2003. Alternative chronologies for Late Quaternary (Last Interglacial–Holocene) deep sea sediments via optical dating of silt-sized quartz. Quat. Sci. Rev. 22 (8–9), 925–941.
Thomas, M.F., Nott, J., Price, D.M., 2001. Late Quaternary stream sedimentation in the humid tropics: a review with new data from NE Queensland, Australia. Geomorphology 39 (1–2), 53–68.
Tucker, G.E., Arnold, L., Bras, R.L., Flores, H., Istanbulluoglu, E., Sólyom, P., 2006. Headwater channel dynamics in semiarid rangelands, Colorado high plains, USA. Geol. Soc. Am. Bull. 118 (7/8), 959–974.
Valentin, C., Poesen, J., Li, Y., 2005. Gully erosion: impacts, factors and control. Catena 63 (2–3), 132–153.
Vandekerckhove, L., Gyssels, G., Poesen, J., Oostwoud Wijdenes, D., 2001. Short-term bank gully retreat rates in Mediterranean environments. Catena 44 (2), 133–161.
Vandekerckhove, L., Poesen, J., Govers, G., 2003. Medium-term gully headcut retreat rates in southeast Spain determined from aerial photographs and ground measurements. Catena 50 (2–4), 329–352.
Wasson, R.J., Galloway, R.W., 1986. Sediment yield in the barrier range before and after European settlement. Aust. Rangel. J. 8 (2), 79–90.
Wasson, R.J., Mazari, R.K., Starr, B., Clifton, G., 1998. The recent history of erosion and sedimentation on the southern tablelands of southeastern Australian: sediment flux dominated by channel incision. Geomorphology 24, 291–308.
Wasson, R.J., Caitcheon, G., Murray, A.S., McCulloch, M., Quade, J., 2002. Sourcing sediment using multiple tracers in the catchment of Lake Argyle, Northwestern Australia. Environ. Manag. 29 (5), 634–646.
Wasson, R.J., Furlonger, L., Parry, D., Pietsch, T., Valentine, E., Williams, D., 2010. Sediment sources and channel dynamics, Daly River, Northern Australia. Geomorphology 114, 161–174.
Waters, C.N., Zalasiewicz, J., Summerhayes, C., Barnosky, A.D., Poirier, C., Gałuszka, A., Cearreta, A., Edgeworth, M., Ellis, E.C., Ellis, M., Jeandel, C., Leinfelder, R., McNeill, J.R., Richter, D.d., Steffen, W., Syvitski, J., Vidas, D., Wagreich, M., Williams, M., Zhisheng, A., Grinevald, J., Odada, E., Oreskes, N., Wolfe, A.P., 2016. The Anthropocene is functionally and stratigraphically distinct from the Holocene. Science 351 (6269).
Wilkinson, J.M., Marshall, L.G., Lundberg, J.G., 2006. River behavior on megafans and potential influences on diversification and distribution of aquatic organisms. J. S. Am. Earth Sci. 21 (1–2), 151–172.
Wilkinson, S.N., Hancock, G.J., Bartley, R., Hawdon, A.A., Keen, R.J., 2013. Using sediment tracing to assess processes and spatial patterns of erosion in grazed rangelands, Burdekin River basin, Australia. Agric. Ecosyst. Environ. 180, 90–102.
Winter, W.H., 1990. Australia's northern savannas: a time for change in management philosophy. J. Biogeogr. 17, 525–529.
Wu, B., Zheng, S., Thorne, C., 2012. A general framework for using the rate law to simulate morphological response to disturbance in the fluvial system. Prog. Phys. Geogr. 36 (5), 575–597.